

ROMANIAN COASTAL DYNAMICS DURING COLD AND WARM SEASONS ANALYZED BY MEANS OF A NUMERICAL MODEL

IRINA DINU¹, MARCO BAJO², GEORG UMGIESSER^{2,3}, ADRIAN STĂNICĂ¹

¹National Institute of Marine Geology and Geo-Ecology (GeoEcoMar), 23-25 Dimitrie Onciul St., 024053 Bucharest, Romania
e-mail: irinadinu@geoecomar.ro, astanica@geoecomar.ro

²Institute of Marine Sciences ISMAR-CNR; Arsenale - Tesa 104, Castello 2737/F, 30122 Venice, Italy
e-mail: marco.bajo@ismar.cnr.it, georg.umgiesser@ismar.cnr.it

³Coastal Research and Planning Institute, CORPI, Klaipeda University; H. Manto 84, LT 92294, Klaipeda, Lithuania
e-mail: georg.umgiesser@ismar.cnr.it

Abstract. The coastal dynamics along the Romanian Black Sea coast is strongly influenced by the wind forcing and by the Danube freshwater and sediment discharge. Temperature and salinity fields may also influence the formation of coastal currents. A 3D hydrodynamic model has been used to analyze the distribution of coastal currents during winter and summer, for the most frequent wind directions and for different values of the Danube discharge. Salinity and calculated fluxes on two representative cross-sections are also compared. The results emphasize the main differences in the hydrodynamics of the Romanian coastal zone, between the winter and the summer period.

Key words: discharge, hydrodynamic model, coastal current, salinity, flux

1. INTRODUCTION

The Romanian Black Sea coastal dynamics is strongly influenced by the wind and the buoyant flow of the Danube water. The effects of the Danube inputs of water and alluvia on the Romanian coastal zone were analyzed by several authors, among whom Panin, 1998; Giosan *et al.*, 1999; Ungureanu and Stănică, 2000; Panin and Jipa, 2002; Stănică *et al.*, 2007; 2011; Stănică and Panin, 2009; Vespremeanu-Stroe *et al.*, 2007; Dan *et al.*, 2007; 2009. A detailed study concerning the influence of the shelfbreak forcing on the Danube buoyant water along the western coast of the Black Sea was performed by Yankovsky *et al.*, 2004. The wind influence on the current circulation is also discussed within this study.

The Romanian coastline is divided into two units, separated by the 5 km long Midia Harbor jetties (Fig. 1), which interrupt the longshore drift of sediments originating from

the Danube river and transported southward, as mentioned by Spătaru, 1990; Panin, 1998; Giosan *et al.*, 1999; Ungureanu and Stănică, 2000. The dynamics of the water and sediments in front of the Danube Delta, as well as the changes induced by humans in the natural coastal evolution were analyzed by several research groups. We can mention the works of Panin, 1998; Giosan *et al.*, 1999; Ungureanu and Stănică, 2000; Stănică *et al.*, 2007; 2011; Stănică and Panin, 2009; Vespremeanu-Stroe *et al.*, 2007; Dan *et al.*, 2007; 2009. In the southern unit of the Romanian coast, the current pathways are influenced mainly by the natural coastal morphology, the coastal structures and the harbor defense works.

The Romanian coastal zone dynamics has been analyzed by means of a 3D hydrodynamic model, named SHYFEM (Shallow Water HYdrodynamic Finite Element Model), which has been implemented on the Black Sea. The SHYFEM model (Umgiesser *et al.*, 2004; Umgiesser, 2010) is developed at the

Institute for Marine Sciences ISMAR-CNR, Venice. The model was applied in several cases around Europe (see e.g. Ferrarin and Umgiesser, 2005; Bellafiore *et al.*, 2008; Ferrarin *et al.*, 2008; De Pascalis *et al.* 2009 and 2012, Umgiesser *et al.*, 2014).

SHYFEM was first used to study the water dynamics along the Romanian coast by Tesconi *et al.*, 2006, focusing on the delta coast between the mouths of Sulina and Sf. Gheorghe distributaries. SHYFEM was also used to analyze the influence of forcing on the formation of coastal currents by Dinu *et al.*, 2011; 2013 and to model the behaviour of the Razelm-Sinoe Lagoon System to forcing (Dinu *et al.*, 2015). Dinu *et al.*, 2013 attempted to compare the available measured currents to the ones provided by the SHYFEM model, in a simplified approach to partially reproduce the wind conditions. This was possible only for some locations. Bajo *et al.*, 2014 showed that the complex dynamics generated along the Romanian coast is due to the interaction of the wind, the Danube freshwater discharge, the sea level, but also of the temperature and salinity distributions. Bajo *et al.*, 2014 also validated the hydrodynamic model for a 2009 dataset, that included sea level, water temperature and CTD profiles.

In this paper, the SHYFEM model is used to compare the Romanian coastal zone dynamics for the cold and warm seasons. To this purpose, the available wind data from the National Administration for Meteorology, from 2005 to 2010, have been used.

2. METHODOLOGY

2.1. THE MODEL

The SHYFEM model (Umgiesser *et al.*, 2004; Umgiesser, 2010) uses a staggered grid, defined by nodes and triangular elements, and a semi-implicit algorithm for the integration in time. The water level is computed at the nodes of the grid, while the velocities are computed at the element centers. The bathymetry is specified in each element. The water column is divided into several layers, the first being the surface layer, while the last is the bottom layer. The layer thicknesses are set by the user and are constant, except for the surface layer, which involves the variation due to the water level.

The Black Sea grid has a gradually increasing resolution towards the shoreline, varying from about 20 km in the central part to about 100 m near the Romanian coast. This resolution can be considered appropriate to solve coastal currents due to meteorological forcing and freshwater discharge.

The model comprises 27 layers. The first 10 m of the water column are divided into 2 m thick layers. Below this depth, the layer thickness increases progressively. The last layer of the model is 500 m thick and extends on a restricted area in the centre of the Black Sea. Open boundary conditions are specified at the Bosphorus Strait and for the main rivers. On the Bosphorus Strait the level is set to zero and the normal fluxes are left free to adjust.

The main river inputs represented in the model are:

- Danube with its distributaries: Chilia, that forms a four-branch secondary delta on the Ukrainian territory, Sulina, and Sf. Gheorghe, in Romania;
- Dnepr, Dnestr, and South Bug, in Ukraine.

The distributaries of the Danube are partially represented in the grid, in order to set up the river momentum when it discharges into the Black Sea. The freshwater inputs are spread among the border elements. The discharge is prescribed and the horizontal velocities are computed by the model. The water discharge for the Danube distributaries was introduced taking into account the percentages provided by Panin, 2003: Chilia 58%, Sulina 19% and Sf. Gheorghe 23%. Other discharge values were introduced in the model for the rivers Dnepr, Dnestr and South Bug, on the territory of Ukraine, and were found in Yankovsky *et al.*, 2004.

Multiannual wind speeds for the winter and summer periods have been calculated based on the available data provided by the Dobrogea Littoral Basin Administration. These data are for the 2004-2010 interval, from several locations along the Romanian coast and one offshore location, the Gloria oil rig (Fig. 1).

The purpose of this study was to compare the coastal dynamics following the winter and summer seasons. As this is a simplified approach, it was reasonable to consider the average of the available wind speeds in the Romanian coastal zone.

For the winter season, the average wind speed along the coast is between $3.1 \text{ m}\cdot\text{s}^{-1}$ at Mangalia and $4.6 \text{ m}\cdot\text{s}^{-1}$ at Gura Portiței, while offshore, at the Gloria oil rig, it is $9 \text{ m}\cdot\text{s}^{-1}$. For the summer season, the average wind speed along the coast is between $2.5 \text{ m}\cdot\text{s}^{-1}$ at Constanța and Eforie, and $3.7 \text{ m}\cdot\text{s}^{-1}$ at Gura Portiței, while offshore, at the Gloria oil rig, it is $6.5 \text{ m}\cdot\text{s}^{-1}$. As it was intended to characterize the Romanian coastal zone, it was reasonable to consider not only the wind speed from the offshore point Gloria, which would have led to exaggerated current velocities, but also the average wind speed in the available points along the coast.

Based on the above-mentioned data, the average wind speeds determined for the Romanian coastal zone are $5 \text{ m}\cdot\text{s}^{-1}$ for the winter season and $4 \text{ m}\cdot\text{s}^{-1}$ for the summer season.

Initial temperature and salinity conditions for the cold and warm seasons were available from the Mediterranean Data Archiving and Rescue (MEDAR) project (<http://medar.ieo.es>). This project provides climatological monthly fields of temperature and salinity for the Mediterranean and the Black Sea obtained from processed observations. The average distributions for the winter and summer periods were interpolated on the Black Sea grid.

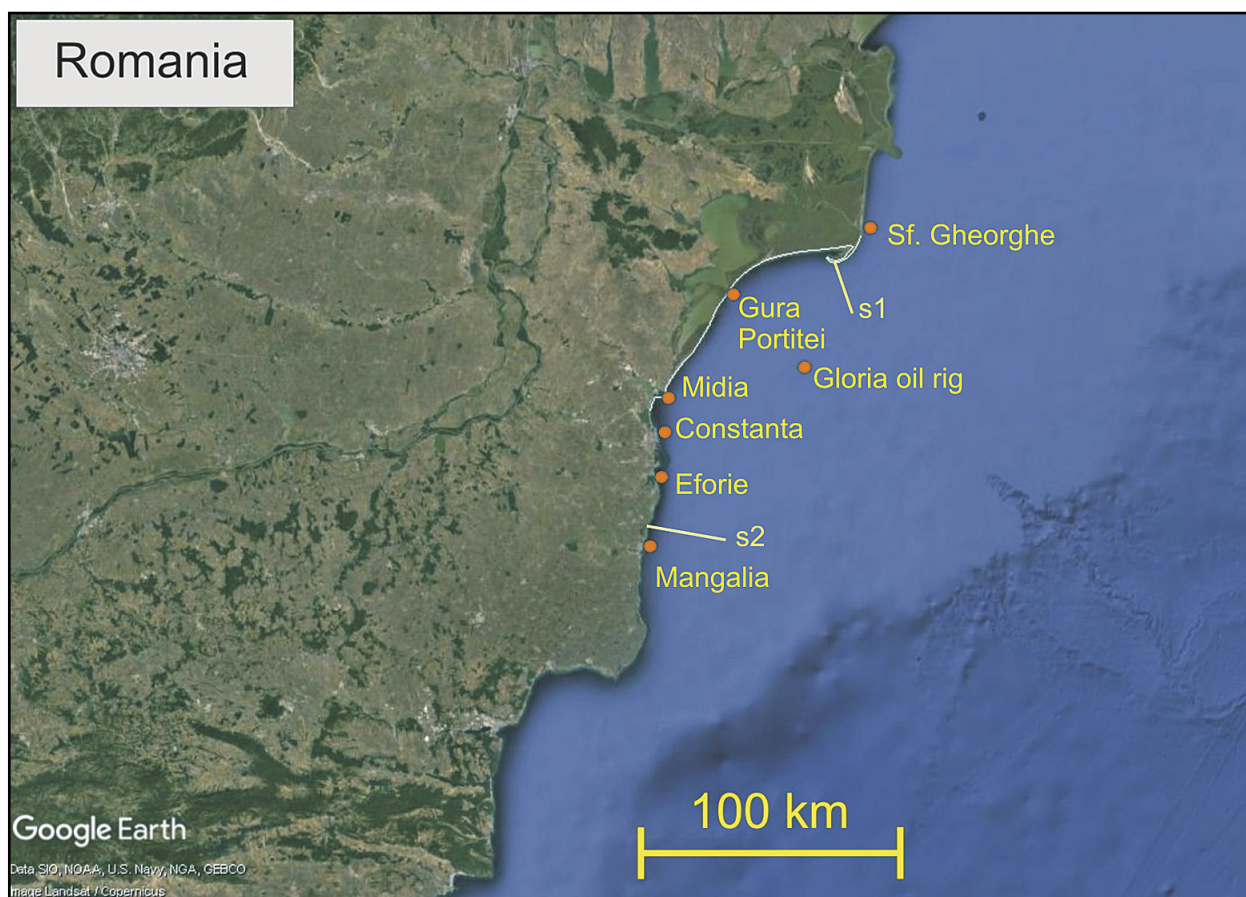


Fig. 1. The Romanian coast with the locations of the observation points (Sf. Gheorghe, Gura Portitei, Midia, Constanta, Eforie, Mangalia, and the offshore point Gloria oil rig); **s1** – the cross-section located South of the Sf. Gheorghe mouth; **s2** – the cross-section located South of Constanta

2.2. SIMULATIONS SETUP

Several simulations have been performed, for the winter and summer seasons, for low, medium and high Danube discharge, and for frequent wind directions parallel to the coast, Northeast and South (Bondar *et al.*, 1973; Bondar and Panin, 2001; Bondar, 2006; HALCROW UK *et al.*, 2011).

For the total Danube discharge, the average value of $6500 \text{ m}^3\cdot\text{s}^{-1}$ was used, provided by Panin and Jipa, 2002. The discharge for the rivers Dnepr, Dnestr and South Bug were 1000 , 400 and $500 \text{ m}^3\cdot\text{s}^{-1}$, respectively, provided by Yankovsky *et al.*, 2004. Other simulations were made imposing the low and high Danube discharge values of $4000 \text{ m}^3\cdot\text{s}^{-1}$ and $15000 \text{ m}^3\cdot\text{s}^{-1}$, respectively, according to the available data from Bondar *et al.*, 1991. The discharges of the rivers Dnepr, Dnestr and South Bug were modified as well, in order to agree with the change of the total Danube discharge. These discharges are presented in Table 1.

3. RESULTS

The results are exposed as distributions of currents and salinity, as well as calculated fluxes on the two cross-sections shown on Figure 1, for all the forcing used, both for the winter and sum-

Table 1. Discharge values introduced in the model

Name	Discharge ($\text{m}^3\cdot\text{s}^{-1}$)		
	minimum	medium	maximum
Prorva (Chilia delta)	400	650	1500
Oceakovsky (Chilia delta)	800	1300	3000
Bystroe (Chilia delta)	480	780	1800
Stari Stambul (Chilia delta)	640	1040	2400
Sulina	760	1235	2850
Sf. Gheorghe	920	1495	3450
<i>Total Danube</i>	<i>4000</i>	<i>6500</i>	<i>15000</i>
Dnepr	600	1000	1500
Dnestr	200	400	600
South Bug	300	500	800

mer seasons. For the SHYFEM model, a cross-section starts from the coast and goes towards offshore. Positive fluxes go to the left of a cross-section, while negative fluxes go to the right. As a consequence, for the cross-sections along the Romanian coastal area, the wind from Northeast will determine a negative flux, while the wind from South will determine a positive flux.

3.1. NE WIND

Currents

The current distributions for all the discharge values considered are presented in Figures 2, 4, 6 for the winter season, and in Figures 8, 10, 12 for the summer season. The salinity distributions for all the discharge values considered are presented in Figures 3, 5, 7 for the winter season, and in Figures 9, 11, 13 for the summer season. Figure 14 shows the calculated fluxes on cross-sections, both for the winter and summer seasons.

The results obtained emphasize a southward long-shore current, visible both in the surface layer and in the deeper layers (Figs. 2, 4, 6).

The current velocities in the surface layer reach values around $50 \text{ cm}\cdot\text{s}^{-1}$ near the Danube mouths, regardless of the Danube discharge (Figs. 2a, 4a, 6a). During the winter period, even for the lowest values of the Danube discharge, of $4000 \text{ m}^3\cdot\text{s}^{-1}$, the current velocities reach values around $50 \text{ cm}\cdot\text{s}^{-1}$ up to 2 m deep, South of the Sf. Gheorghe mouth (Fig. 2c). For the medium Danube discharge of $6500 \text{ m}^3\cdot\text{s}^{-1}$, the current velocities reach values around $50 \text{ cm}\cdot\text{s}^{-1}$ up to 4 m deep, south of the Sf. Gheorghe mouth (Fig. 4c). For the highest discharge, of $15000 \text{ m}^3\cdot\text{s}^{-1}$, the current velocities reach values around $50 \text{ cm}\cdot\text{s}^{-1}$ even at 5 m deep (Fig. 6b, c).

The currents are weaker for the summer period. For the lowest values of the Danube discharge, of $4000 \text{ m}^3\cdot\text{s}^{-1}$, the current velocities reach values under $50 \text{ cm}\cdot\text{s}^{-1}$ up to 2 m deep, South of the Sf. Gheorghe mouth (Fig. 8c). For the medium Danube discharge of $6500 \text{ m}^3/\text{s}$, the current velocities reach values around $50 \text{ cm}\cdot\text{s}^{-1}$ up to 2 m deep, South of the Sf. Gheorghe mouth (Fig. 10c). For the increased Danube discharge of $15000 \text{ m}^3\cdot\text{s}^{-1}$, the current velocities reach values around $50 \text{ cm}\cdot\text{s}^{-1}$ up to 2.5 m deep, South of the Sf. Gheorghe mouth (Fig. 12c).

Salinity

The salinity is influenced by the Danube discharge and also by the season, as the initial salinity distributions differ for the winter and summer periods. For the winter period, the zone of minimum salinity of 13 psu is more extended, as the Danube discharge increases (Figs. 3a, 5a, and 7a). For the increased Danube discharge of $15000 \text{ m}^3\cdot\text{s}^{-1}$, the zone of minimum salinity may exceed 5 m deep, as shown in Figure 7b. For the summer period, the distribution of sa-

linity is significantly changed, due to the influence of the initial temperature and salinity fields (Figs. 9a, 11a, and 13a). The cross-section located South of the Sf. Gheorghe mouth shows that the zone of minimum salinity reaches 10 m deep, regardless of the Danube discharge (Figs. 9b, 11b and 13b).

As previously discussed by Yankovsky *et al.*, 2004 for a summer period dataset, the NE wind is downwelling-favourable and tends to deepen the buoyant water. This is emphasized by the salinity cross-sections provided by the model, for the summer period (Figs. 9, 11 and 13).

Fluxes

The calculated fluxes on the cross-sections located South of Sf. Gheorghe and South of Constanța (Fig. 14 and Tables 2 and 3) are significantly higher for the winter period. This is influenced by the slightly higher value of the average NE wind speed for the winter period. For every Danube discharge considered, one can notice that the zones of higher current velocities are more extended for the winter period, both in surface and in depth (Fig. 2 vs. Fig. 8, Fig. 4 vs. Fig. 10 and Fig. 6 vs. Fig. 12).

Table 2. Winter and summer fluxes ($\text{m}^3\cdot\text{s}^{-1}$) calculated for the cross-section located South of the Sf. Gheorghe mouth for NE wind

Danube discharge ($\text{m}^3\cdot\text{s}^{-1}$)	winter	summer
4000	- 48903.50	- 26804.42
6500	- 53206.49	- 30390.56
15000	- 64949.21	- 41545.86

Table 3. Winter and summer fluxes ($\text{m}^3\cdot\text{s}^{-1}$) calculated for the cross-section located South of Constanța for NE wind

Danube discharge ($\text{m}^3\cdot\text{s}^{-1}$)	winter	summer
4000	- 126981.85	- 37688.14
6500	- 130159.48	- 42059.64
15000	- 139414.44	- 55318.55

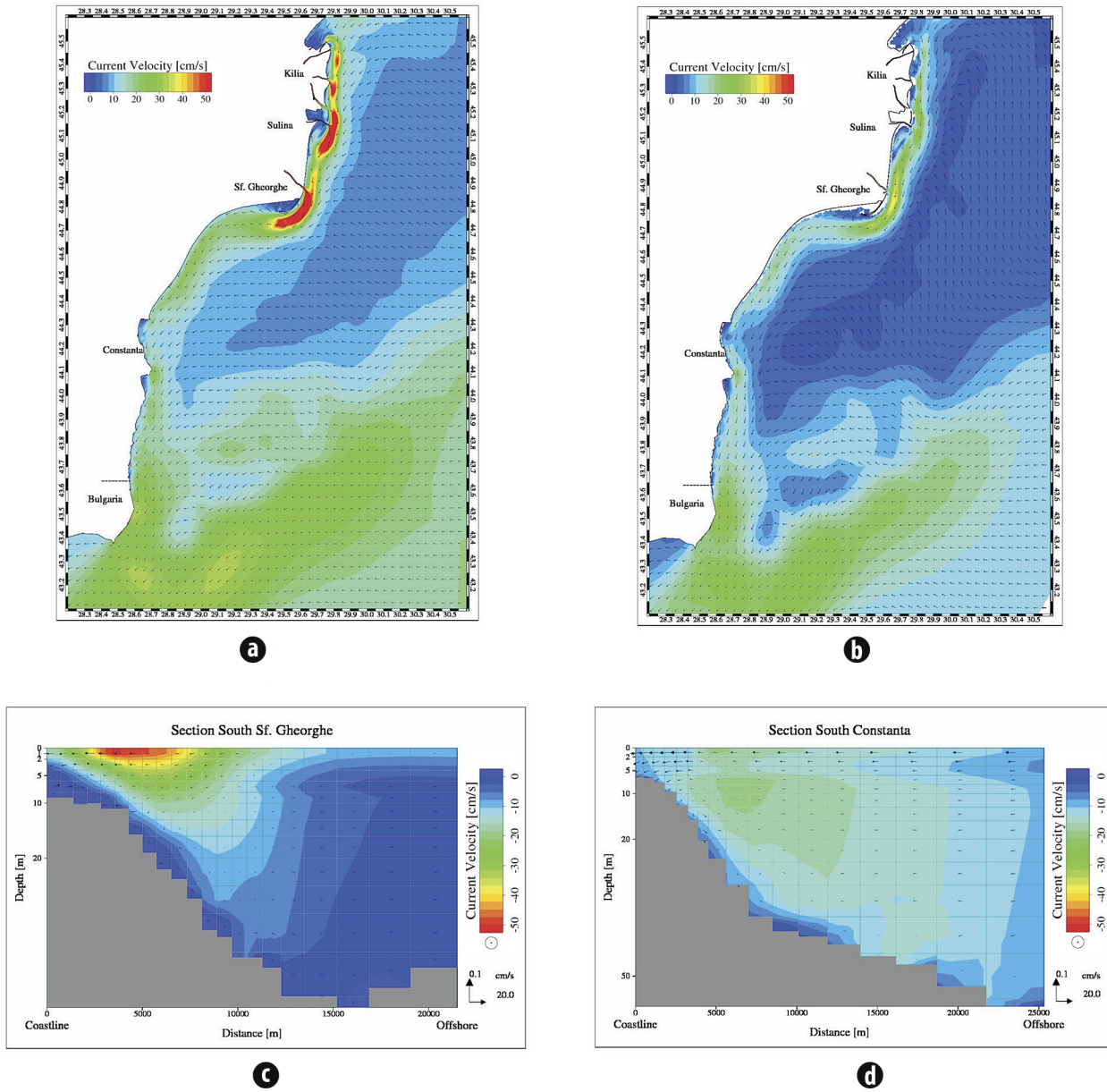


Fig. 2. Distribution of currents for NE wind and low discharge, winter season: **a)** in the surface layer; **b)** at 5 m deep; **c)** cross-section located South of the Sf. Gheorghe mouth; **d)** cross-section located South of Constanța

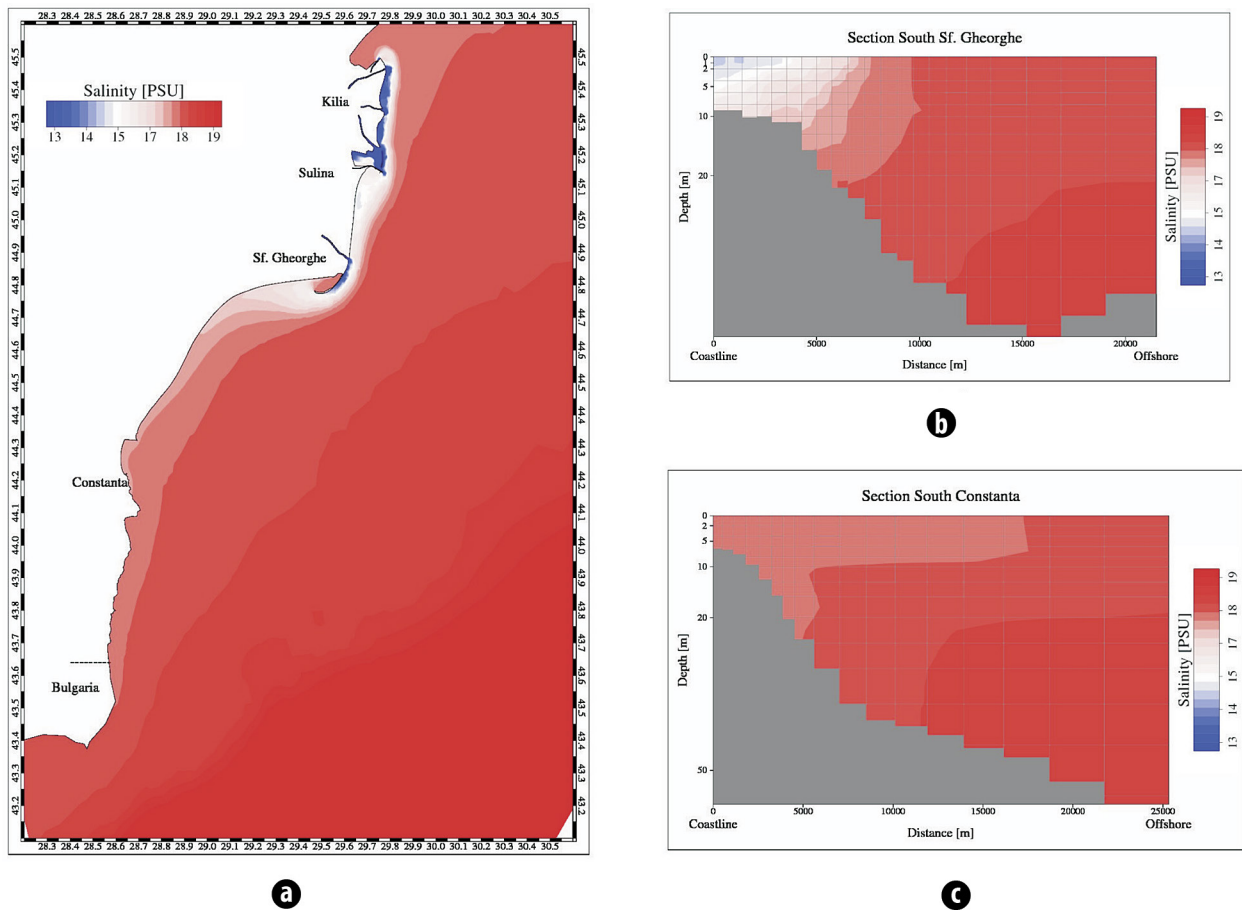


Fig. 3. Distribution of salinity for NE wind and low discharge, winter season: **a)** in surface; **b)** cross-section located South of the Sf. Gheorghe mouth; **c)** cross-section located South of Constanța

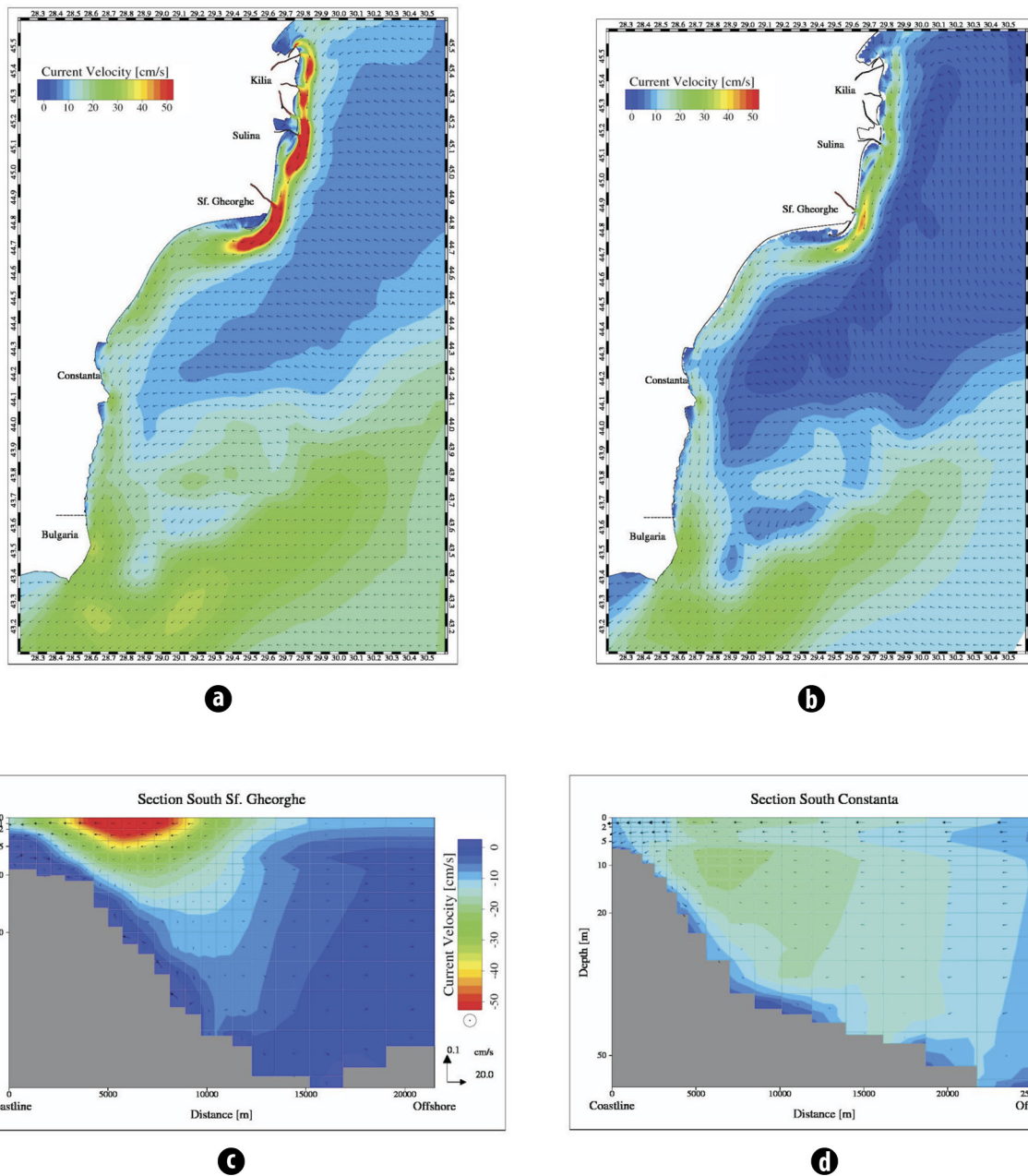


Fig. 4. Distribution of currents for NE wind and medium discharge, winter season: **a)** in the surface layer; **b)** at 5 m deep; **c)** cross-section located South of the Sf. Gheorghe mouth; **d)** cross-section located South of Constanța

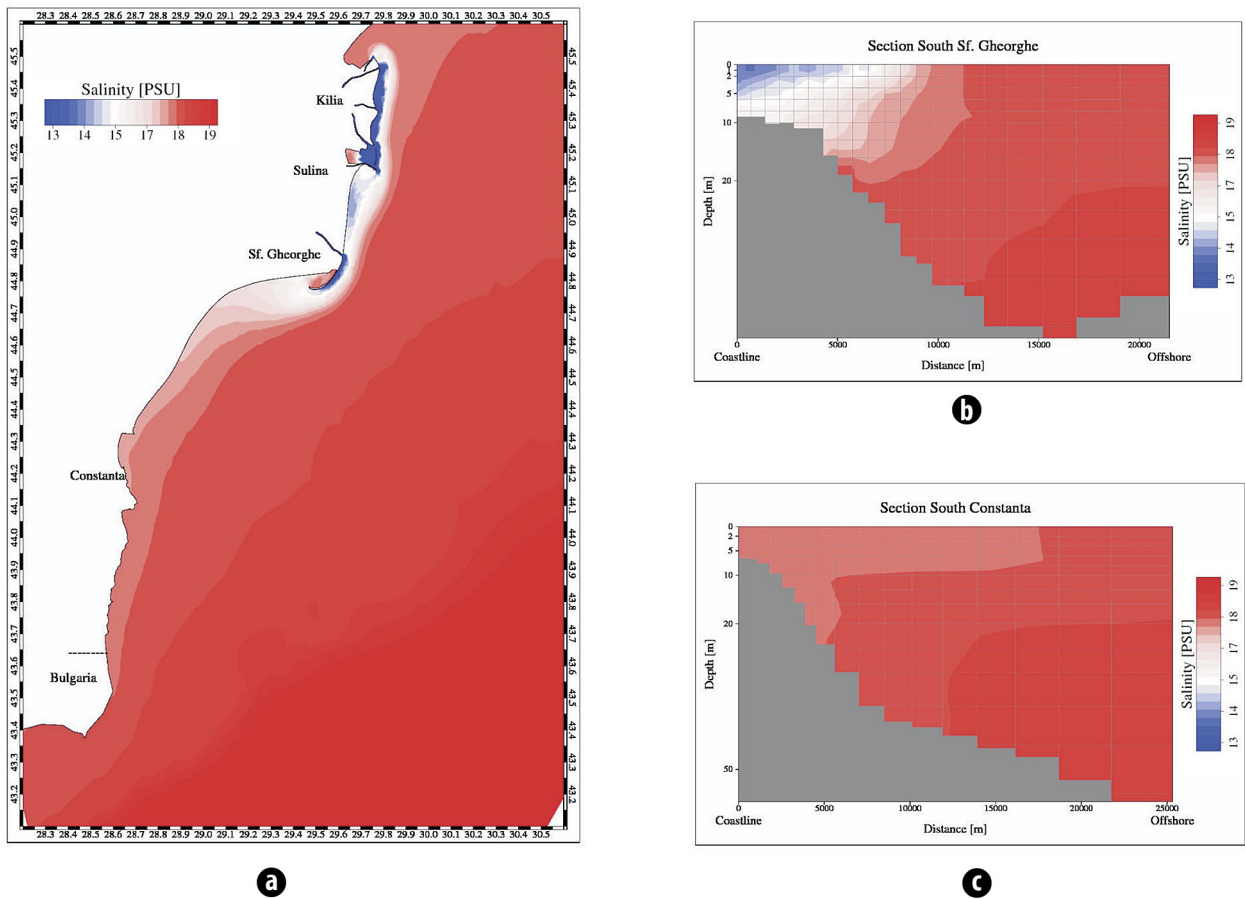


Fig. 5. Distribution of salinity for NE wind and medium discharge, winter season: **a)** in surface; **b)** cross-section located South of the Sf. Gheorghe mouth; **c)** cross-section located South of Constanța

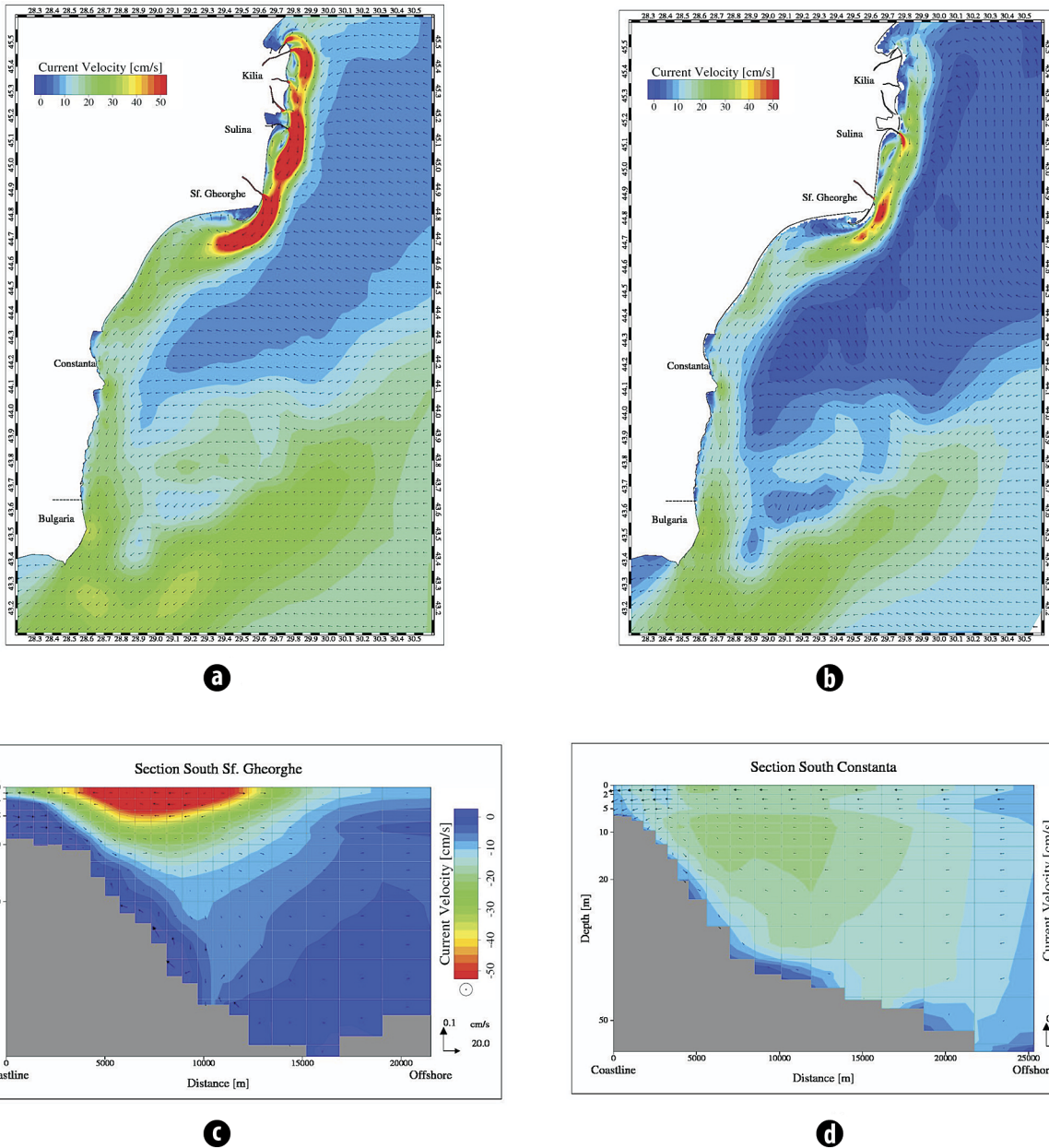


Fig. 6. Distribution of currents for NE wind and high discharge, winter season: **a)** in the surface layer; **b)** at 5 m deep; **c)** cross-section located South of the Sf. Gheorghe mouth; **d)** cross-section located South of Constanța

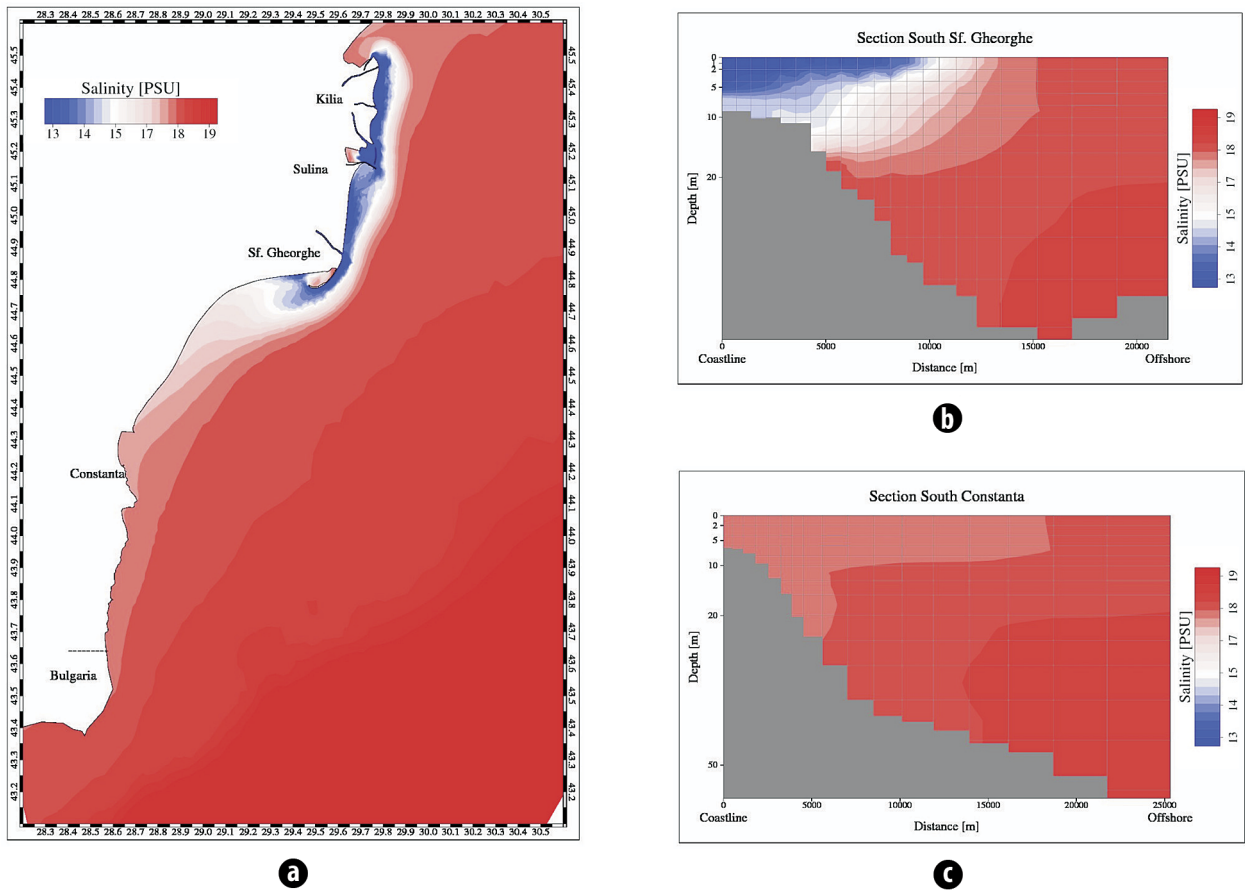


Fig. 7. Distribution of salinity for NE wind and high discharge, winter season: **a)** in surface; **b)** cross-section located South of the Sf. Gheorghe mouth; **c)** cross-section located South of Constanța

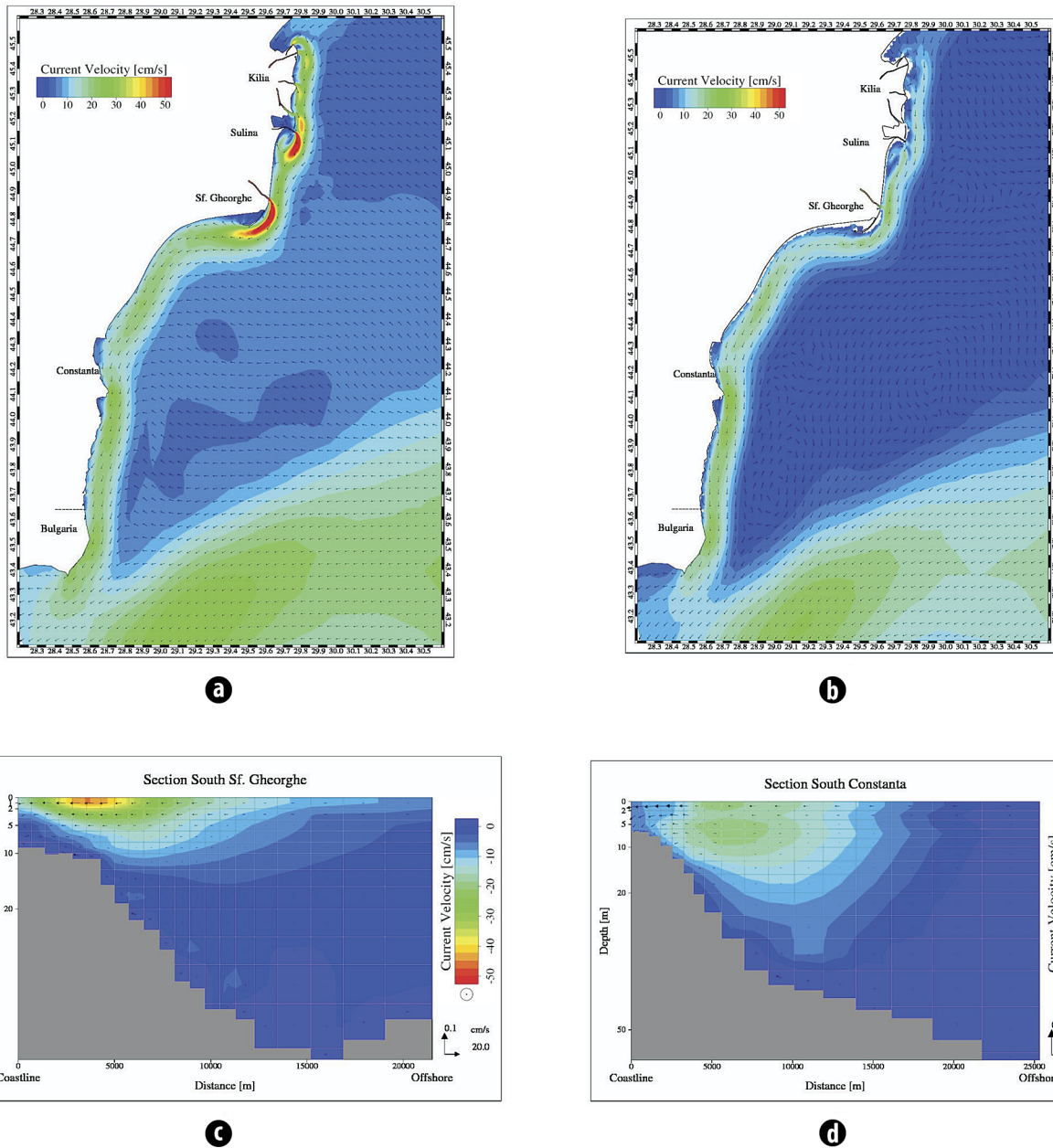


Fig. 8. Distribution of currents for NE wind and low discharge, summer season: **a)** in the surface layer; **b)** at 5 m deep; **c)** cross-section located South of the Sf. Gheorghe mouth; **d)** cross-section located South of Constanța

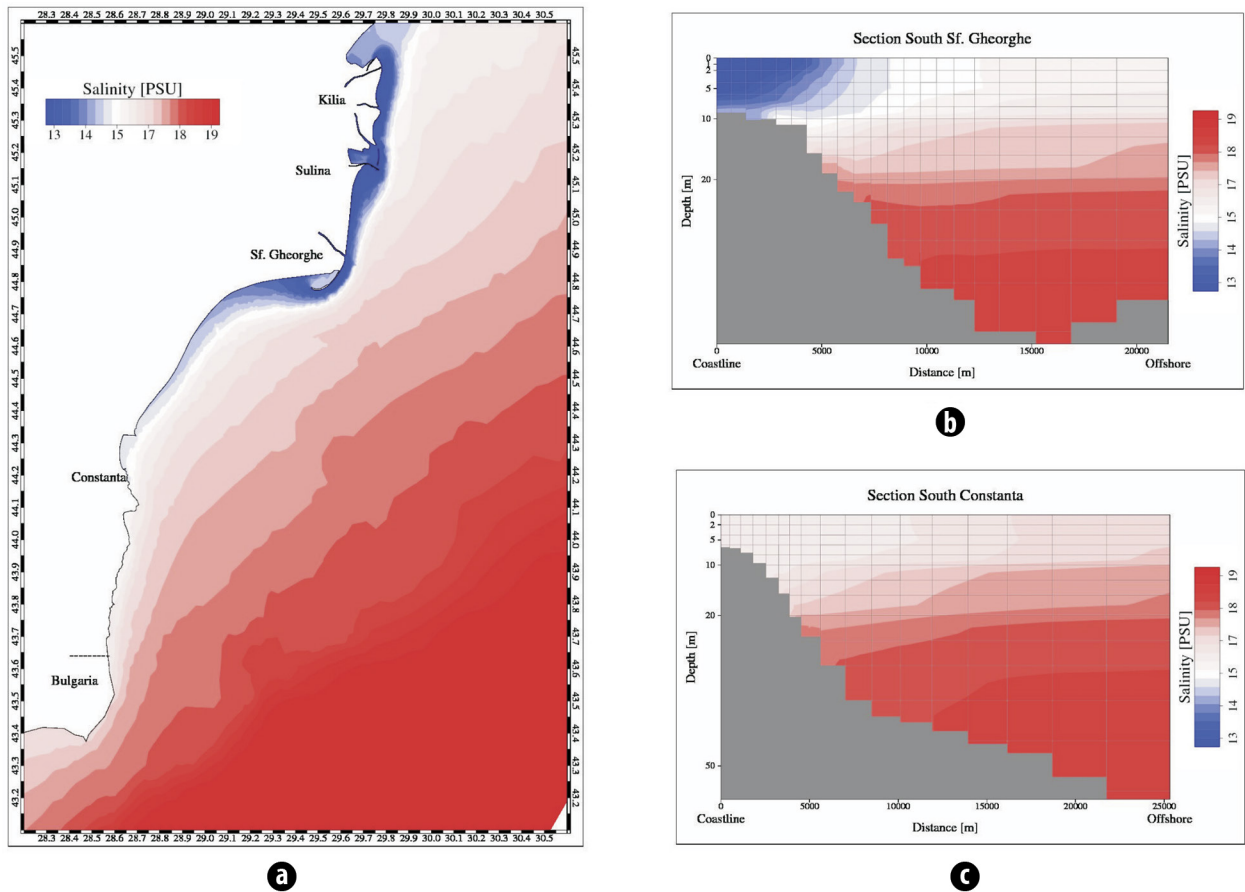


Fig. 9. Distribution of salinity for NE wind and low discharge, summer season: **a)** in surface; **b)** cross-section located South of the Sf. Gheorghe mouth; **c)** cross-section located South of Constanța

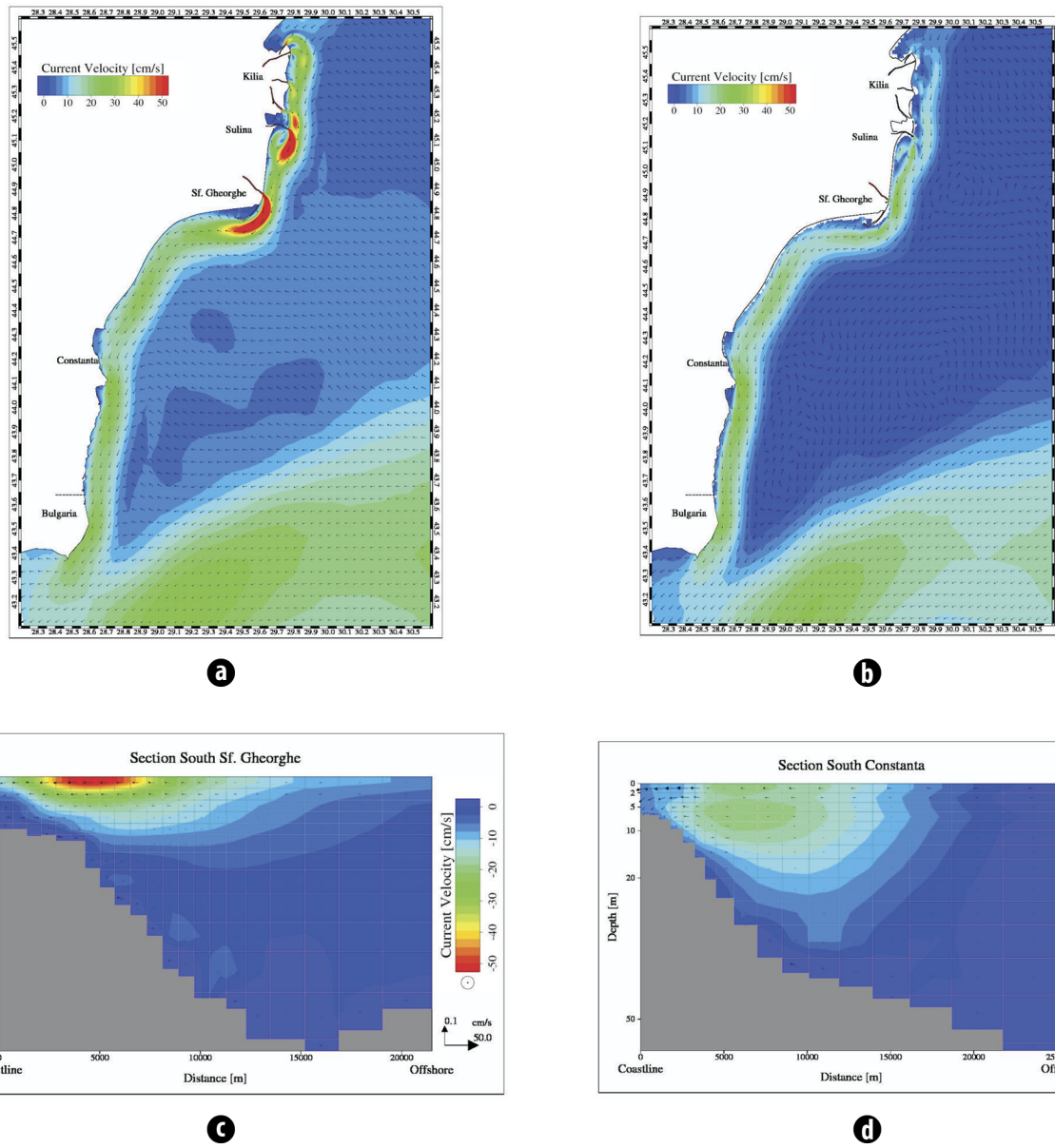


Fig. 10. Distribution of currents for NE wind and medium discharge, summer season: **a)** in the surface layer; **b)** at 5 m deep; **c)** cross-section located South of the Sf. Gheorghe mouth; **d)** cross-section located South of Constanța

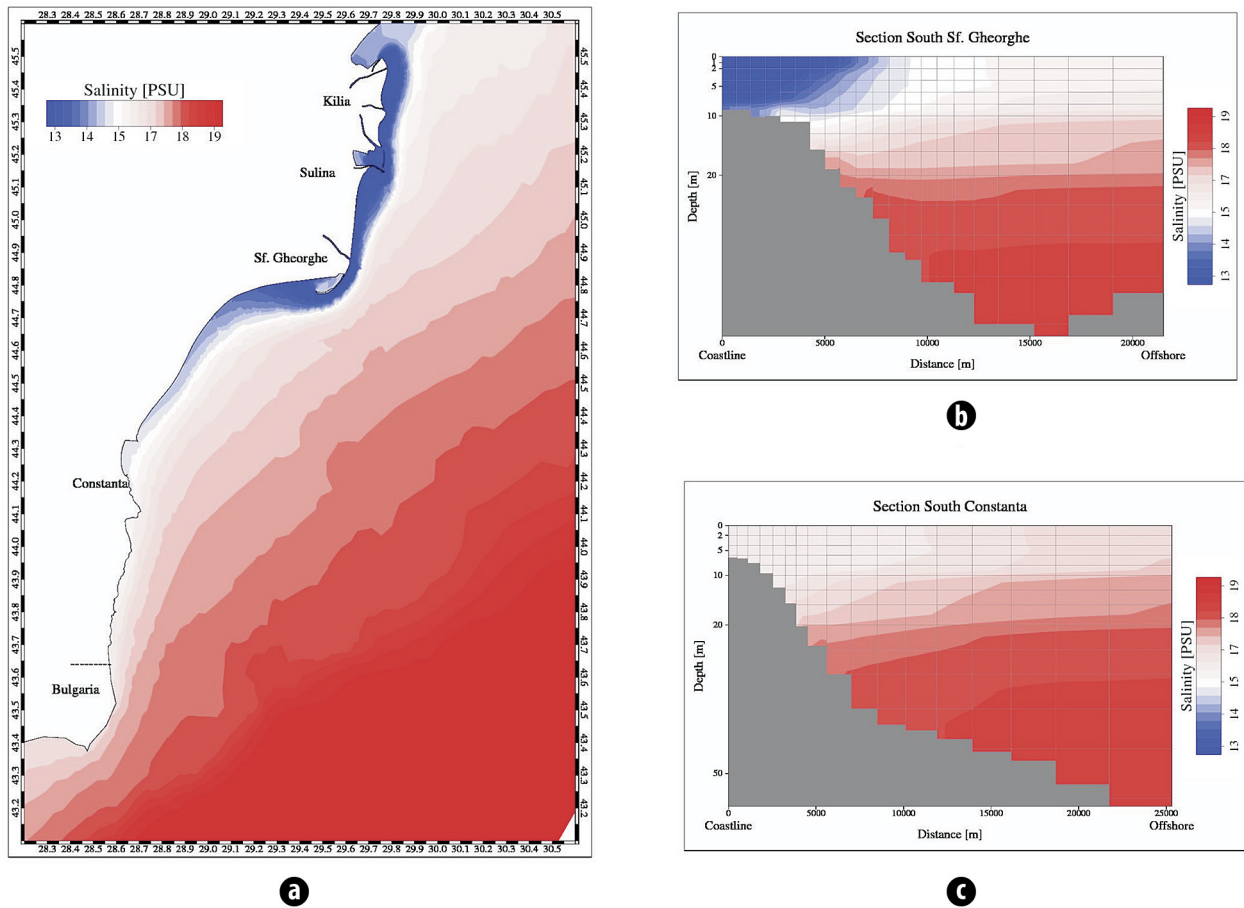


Fig. 11. Distribution of salinity for NE wind and medium discharge, summer season: **a)** in surface; **b)** cross-section located South of the Sf. Gheorghe mouth; **c)** cross-section located South of Constanța

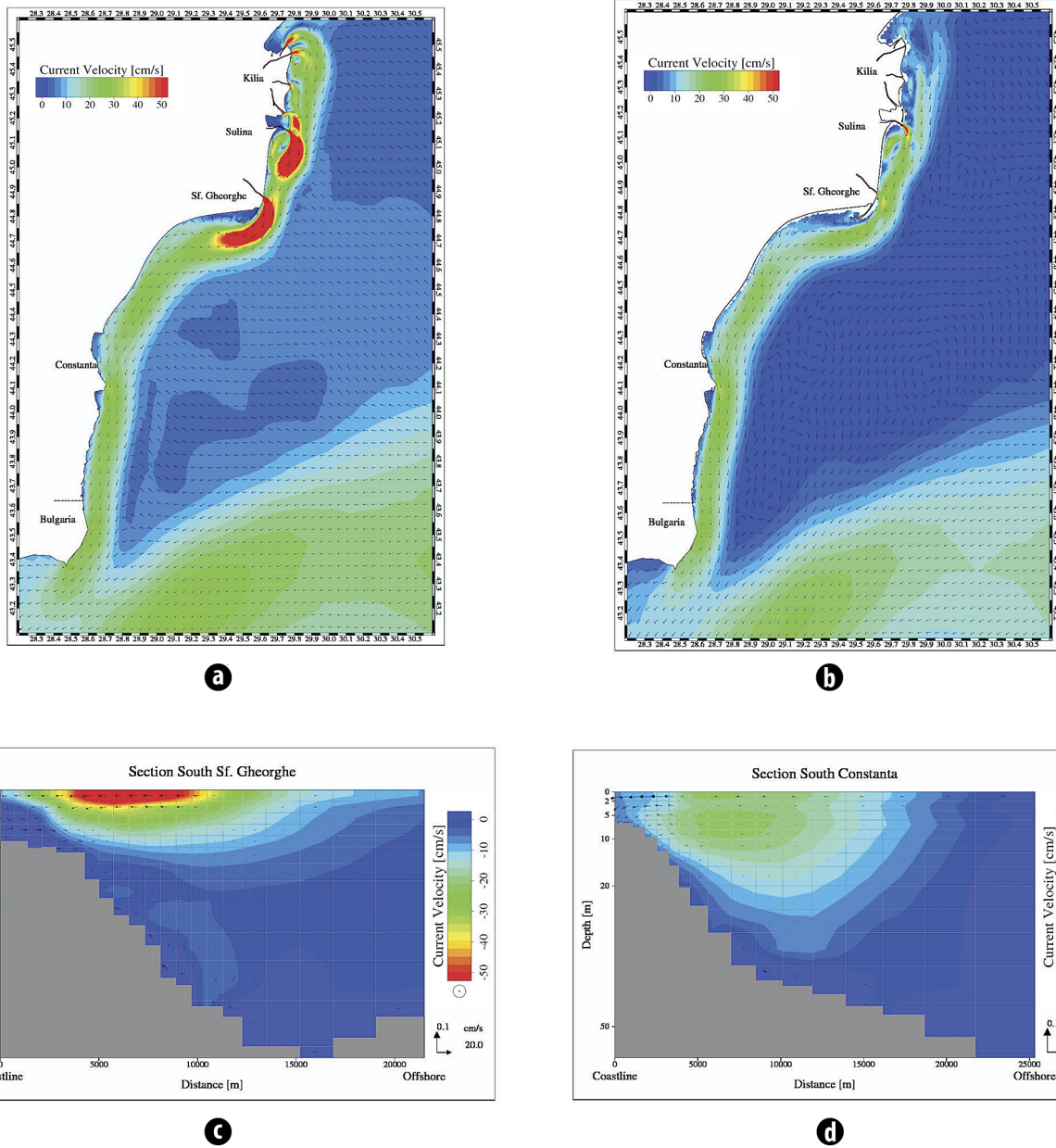


Fig. 12. Distribution of currents for NE wind and high discharge, summer season: **a)** in the surface layer; **b)** at 5 m deep; **c)** cross-section located South of the Sf. Gheorghe mouth; **d)** cross-section located South of Constanța

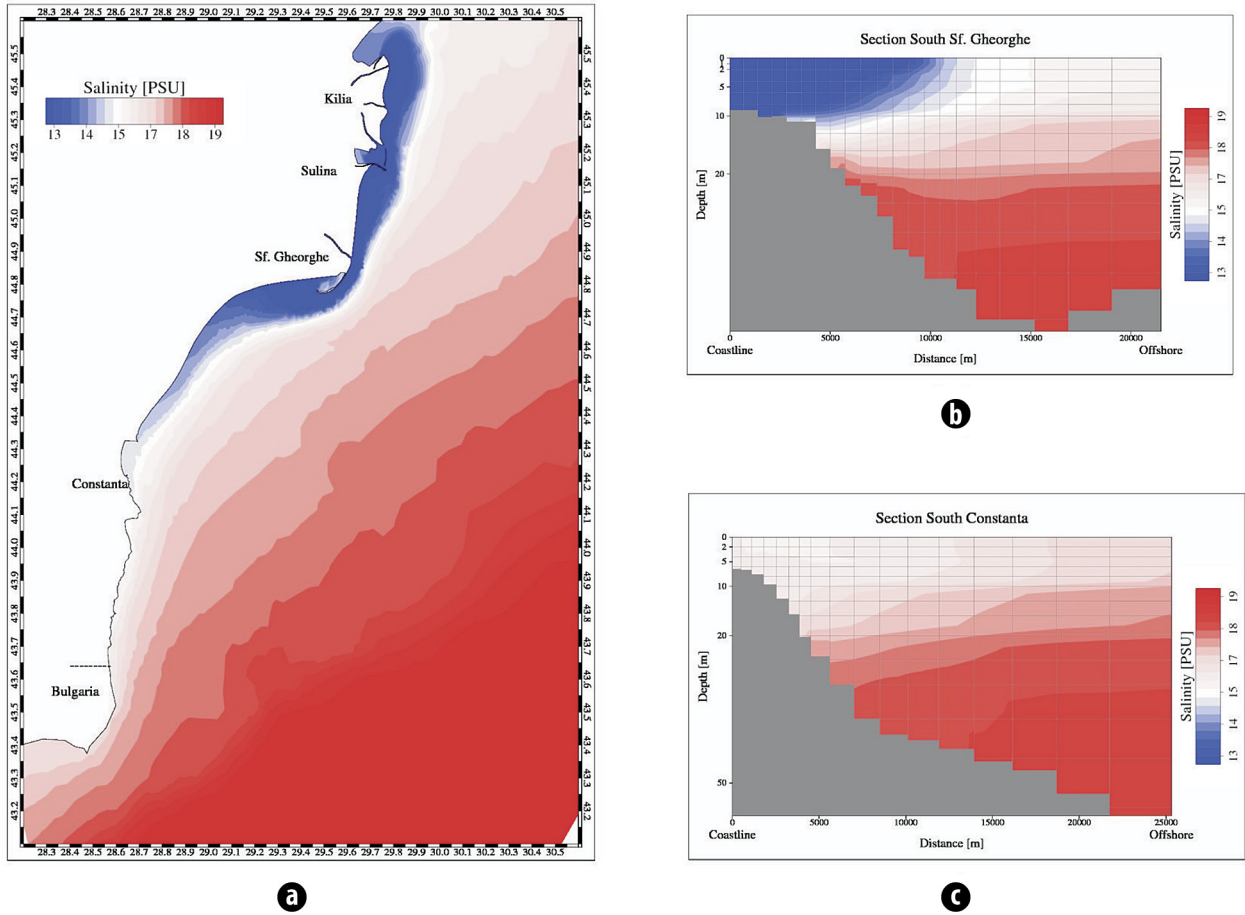


Fig. 13. Distribution of salinity for NE wind and high discharge, summer season: **a)** in surface; **b)** cross-section located South of the Sf. Gheorghe mouth; **c)** cross-section located South of Constanța

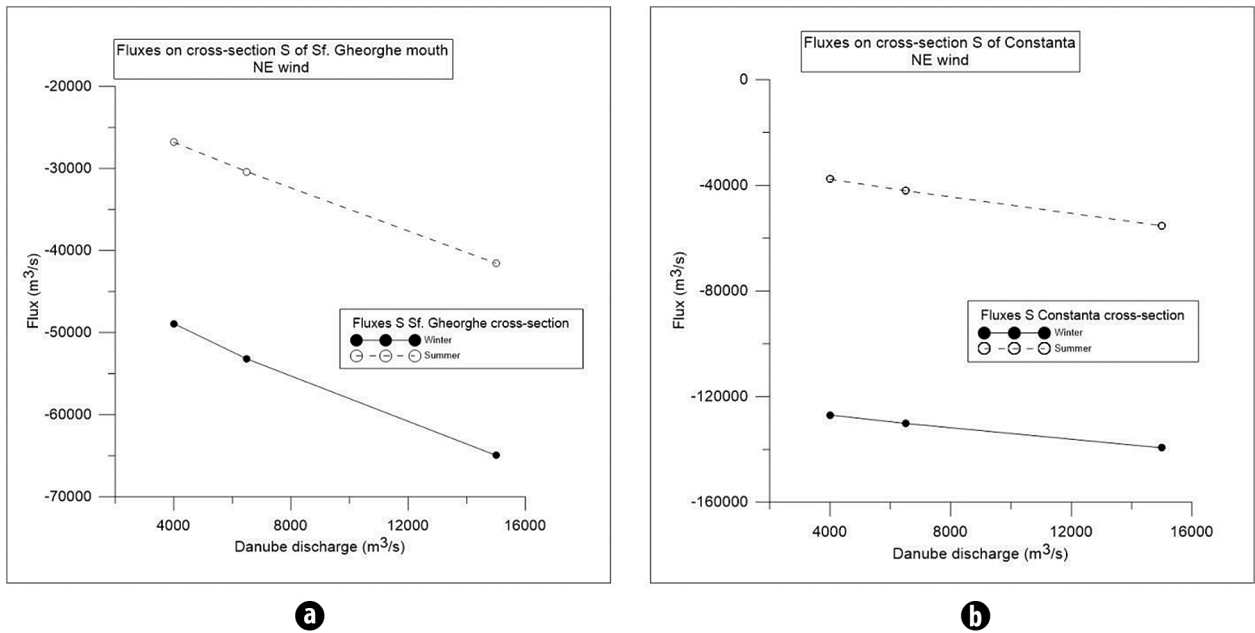


Fig. 14. Calculated fluxes for NE wind on: **a)** the cross-section located South of the Sf. Gheorghe mouth; **b)** the cross-section located South of Constanța

3.2. S WIND

Currents

The current distributions for all the discharge values considered are presented in Figures 15, 17, 19 for the winter season, and in Figures 21, 23, 25 for the summer season. The salinity distributions for all the discharge values considered are presented in Figures 16, 18, 20 for the winter season, and in Figures 22, 24, 26 for the summer season. Figure 27 shows the calculated fluxes on cross-sections, both for the winter and summer seasons.

The results obtained emphasize a northward longshore current, which is weaker than for the simulations forced with NE wind. For the medium Danube discharge of $6500 \text{ m}^3\cdot\text{s}^{-1}$, the surface current velocities reach values around $50 \text{ cm}\cdot\text{s}^{-1}$ only on a very restricted area around the Sulina mouth, both for the winter and summer periods (Figs. 17a and 23a). For the increased Danube discharge of $15000 \text{ m}^3\cdot\text{s}^{-1}$, the surface current velocities reach values around $50 \text{ cm}\cdot\text{s}^{-1}$ in the zones of all the Danube mouths, both for the winter and summer periods (Figs. 19a and 25a), but these zones are significantly smaller than for the simulations forced with wind from NE.

As the wind from South opposes the downdrift propagation of the buoyant Danube flow, the current velocities are lower than for the simulations forced with wind from NE. Even if the Danube discharge increases, the wind from South pushes the Danube freshwater towards North (Figs. 15, 17 and 19 for the winter period and Figs. 21, 23 and 25 for the summer period). As a consequence, the current velocities are weaker, both in surface and in the deeper layers. For higher discharge, the zone with increased current velocities is more reduced and moved offshore. This is best shown in the cross-section located South of the Sf. Gheorghe mouth and it occurs both for the winter and summer periods (Figs. 15c, 17c, 19c, 21c, 23c and 25c). It also agrees with the conclusions of previous studies, that wind is the main factor controlling the overall circulation in the Romanian coastal zone (Dinu *et al.*, 2011; 2013).

Salinity

For the winter period, zones of low salinity appear only in the areas of the Danube mouths (Figs. 16a, 18a, and 20a). They are more extended for the increased value of the Danube discharge (Fig. 20a). The salinity cross-section located South of the Sf. Gheorghe mouth is more uniform than for NE wind, while the salinity cross-section located South of Constanța is the same, even for the increased Danube discharge (Figs. 16b, 16c, 18b, 18c, 20b and 20c).

The situation is different for the summer period. As the Danube buoyant water is pushed towards offshore, the zones of minimum salinity are less extended comparing with the

ones provided by the simulations forced with NE wind, even for the increased Danube discharge (Figs. 22a, 24a and 26a). The stratification is weaker comparing to the results of the simulations forced with NE wind. For the increased Danube discharge of $15000 \text{ m}^3\cdot\text{s}^{-1}$, on the cross-section located South of the Sf. Gheorghe mouth, the zone of minimum salinity, of 13 psu, reaches 5 m deep near the coast and extends up to 5 km offshore (Fig. 26b). For the same Danube discharge and the same cross-section, the zone of minimum salinity reaches 10 m deep and extends almost 10 km offshore in the case of NE wind (Fig. 13b). Meanwhile, the cross-section located South of Constanța shows low variability, even at the highest Danube discharge considered (Figs. 22c, 24c and 26c).

Fluxes

The calculated fluxes on the cross-sections located South of Sf. Gheorghe and South of Constanța (Fig. 27 and Tables 4 and 5) are significantly different for the winter and summer periods. For the winter period, and for low and medium Danube discharge, the fluxes calculated for the cross-section located South of the Sf. Gheorghe mouth are positive (Table 4). For the winter period, and for the increased Danube discharge of $15000 \text{ m}^3\cdot\text{s}^{-1}$, the fluxes are negative (Table 4). This happens because the above-mentioned cross-section is located at the end of the Sahalin spit and the Danube buoyant flow is still strong enough to oppose the effect of the wind from South. For the summer simulations, all the fluxes calculated on the cross-section located South of Sf. Gheorghe are positive (northward). However, for the increased Danube discharge of $15000 \text{ m}^3\cdot\text{s}^{-1}$, the northward flux has the lowest value (Table 4 and Fig. 27a).

The calculated fluxes on the cross-section located South of Constanța are negative for the winter period and positive for the summer period (Table 5). For the winter period and for all the Danube discharge values, a narrow strip, parallel to the coast, with northward current can be noticed in the surface layer, while towards offshore, the main current direction is southward (negative) (Figs. 15a, 17a and 19a). In the deeper layers, the current directions are also southward, thus resulting in negative fluxes on this cross-section (Figs. 15b, 17b, and 19b). Northward (positive) fluxes during the summer period occur because a stronger northward longshore current is formed, mostly due to the influence of the temperature and salinity distributions (Dinu *et al.*, 2011; 2013). This can be seen in the current distributions provided by the model, for the winter and summer periods, for wind from South and for all the Danube discharge considered. The width of the zone parallel to the coast, with increased current velocities, is larger for the summer period simulations (Figs. 15a vs 21a for low discharge; Figs. 17a vs 23a for medium discharge; and Figs. 19a vs 25a for the highest discharge).

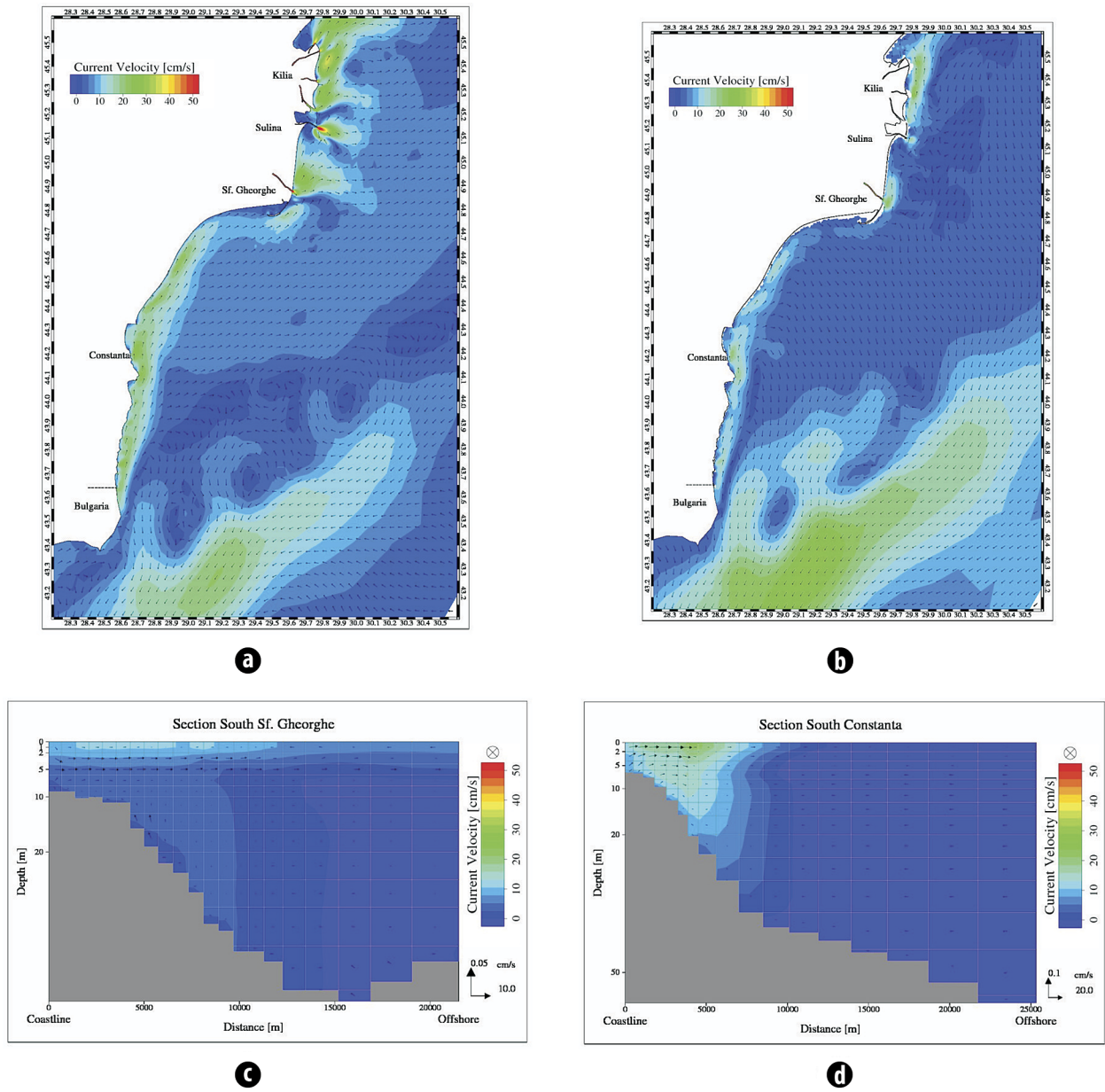


Fig. 15. Distribution of currents for S wind and low discharge, winter season: **a)** in the surface layer; **b)** at 5 m deep; **c)** cross-section located South of the Sf. Gheorghe mouth; **d)** cross-section located South of Constanța.

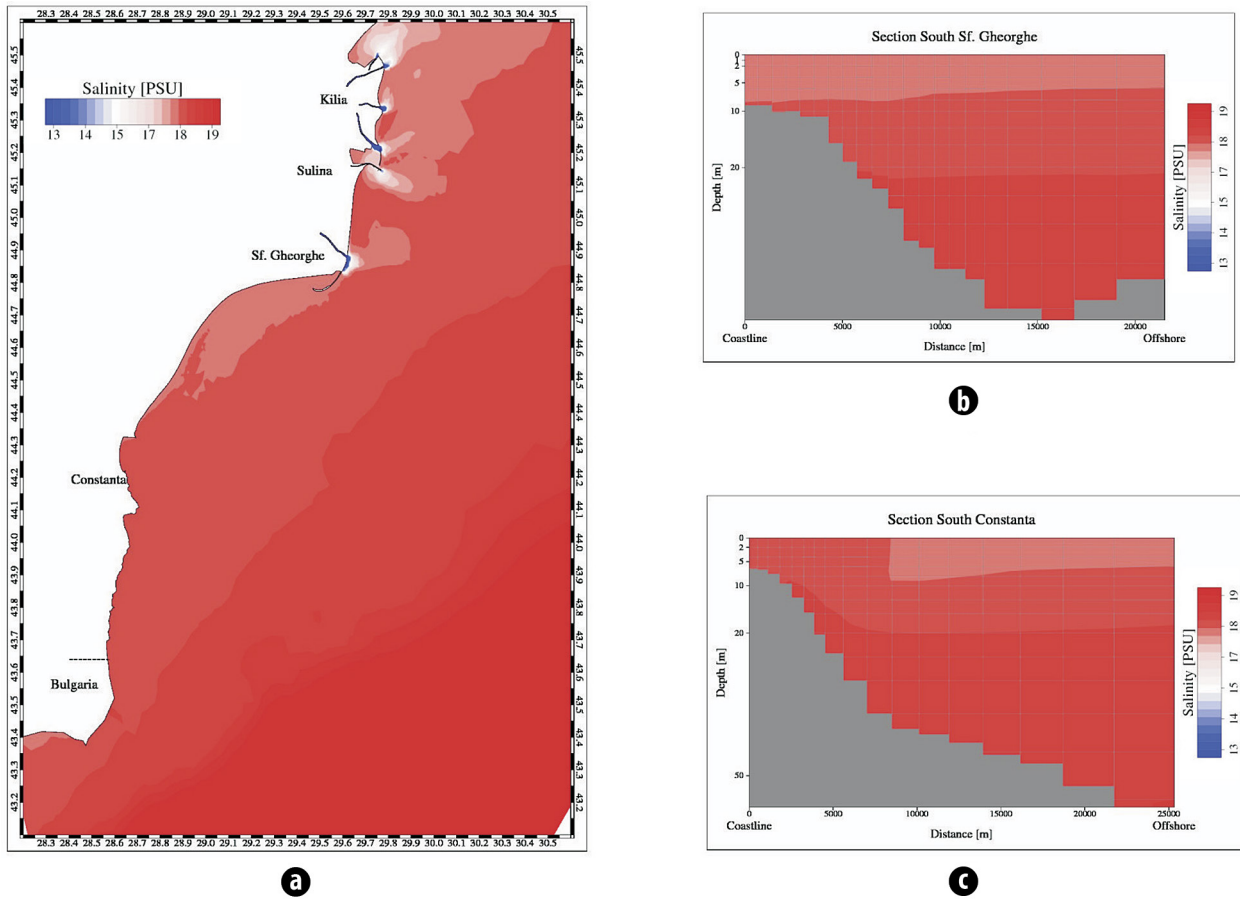


Fig. 16. Distribution of salinity for S wind and low discharge, winter season: **a)** in surface; **b)** cross-section located South of the Sf. Gheorghe mouth; **c)** cross-section located South of Constanța

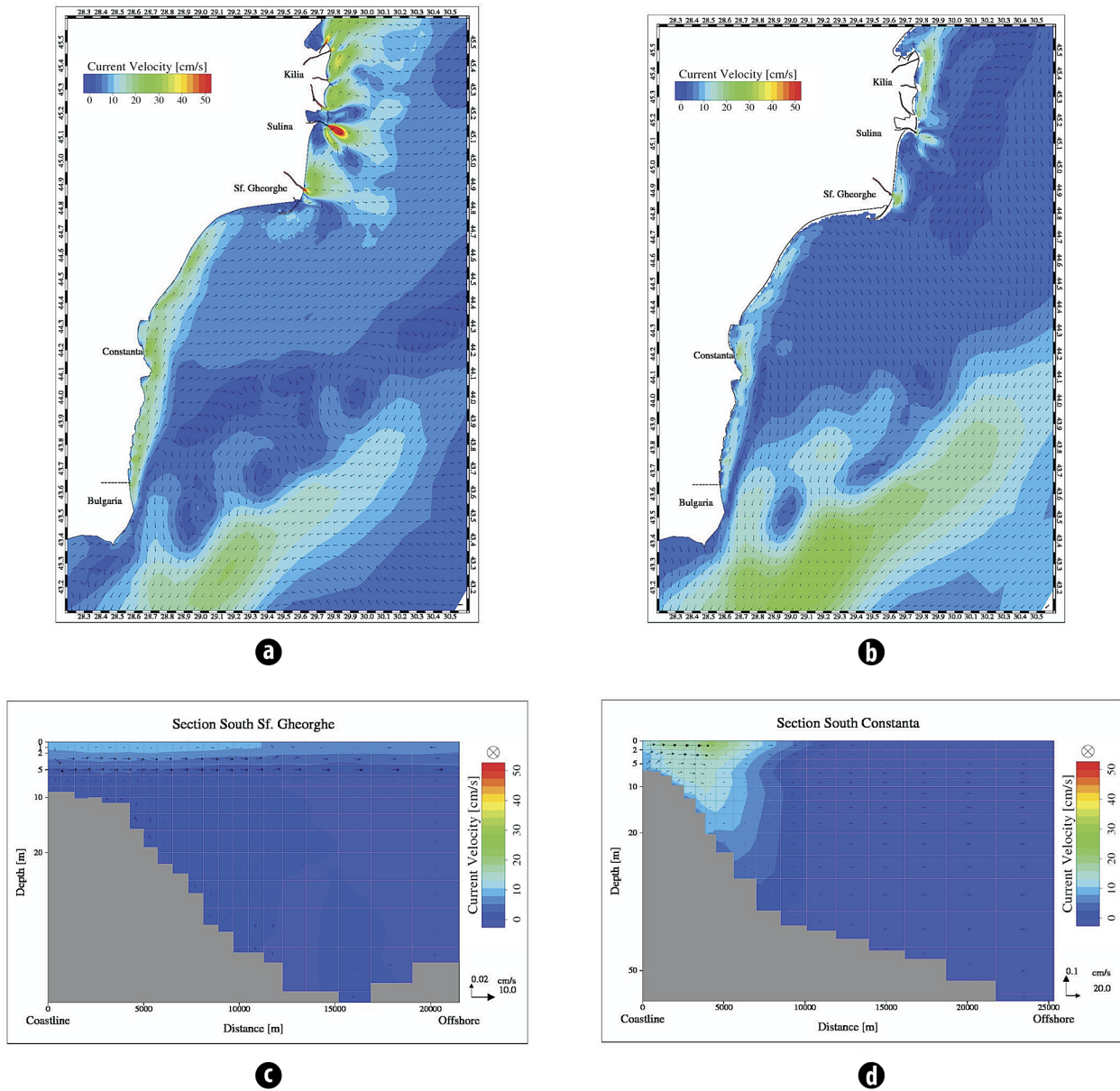


Fig. 17. Distribution of currents for S wind and medium discharge, winter season: **a)** in the surface layer; **b)** at 5 m deep; **c)** cross-section located South of the Sf. Gheorghe mouth; **d)** cross-section located South of Constanța

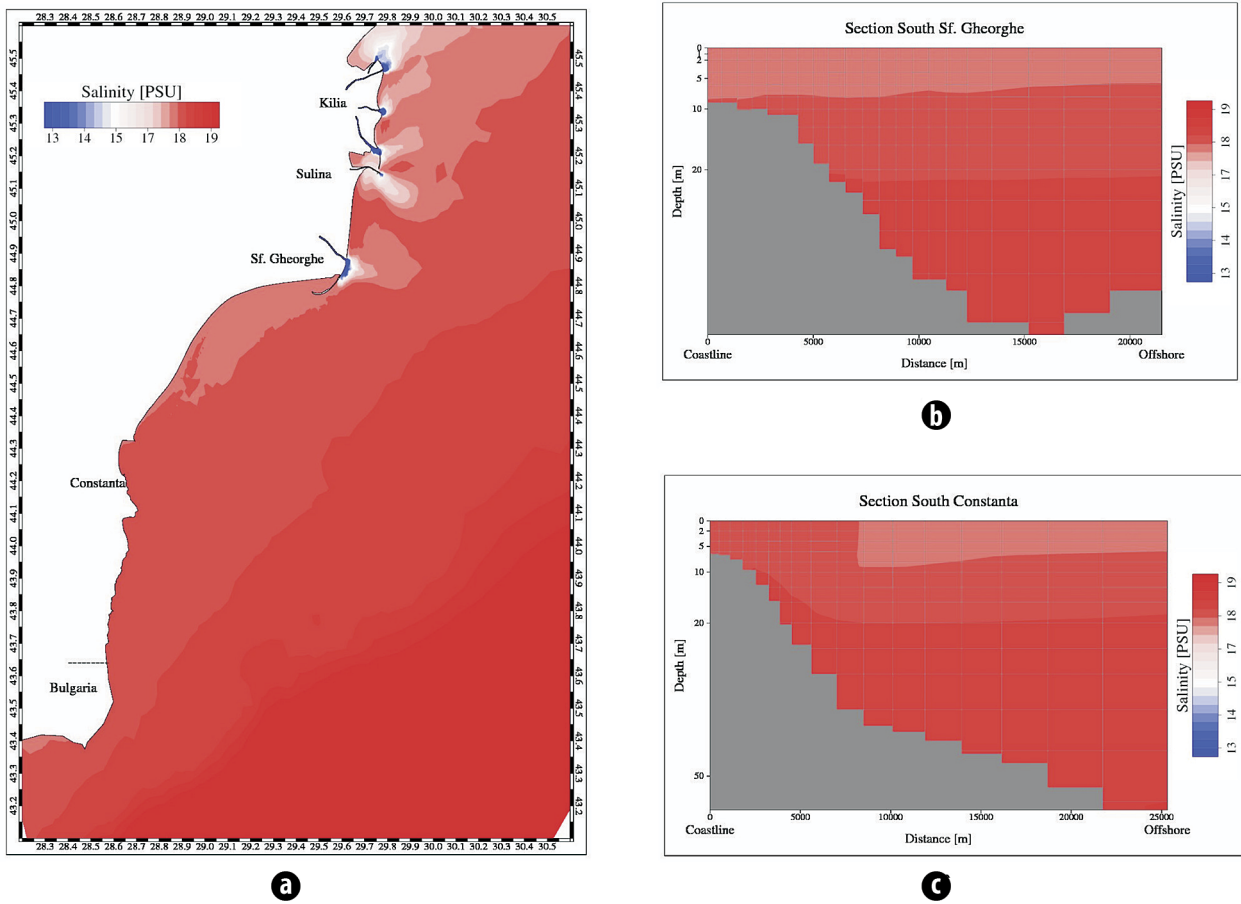


Fig. 18. Distribution of salinity for S wind and medium discharge, winter season: **a)** in surface; **b)** cross-section located South of the Sf. Gheorghe mouth; **c)** cross-section located South of Constanța

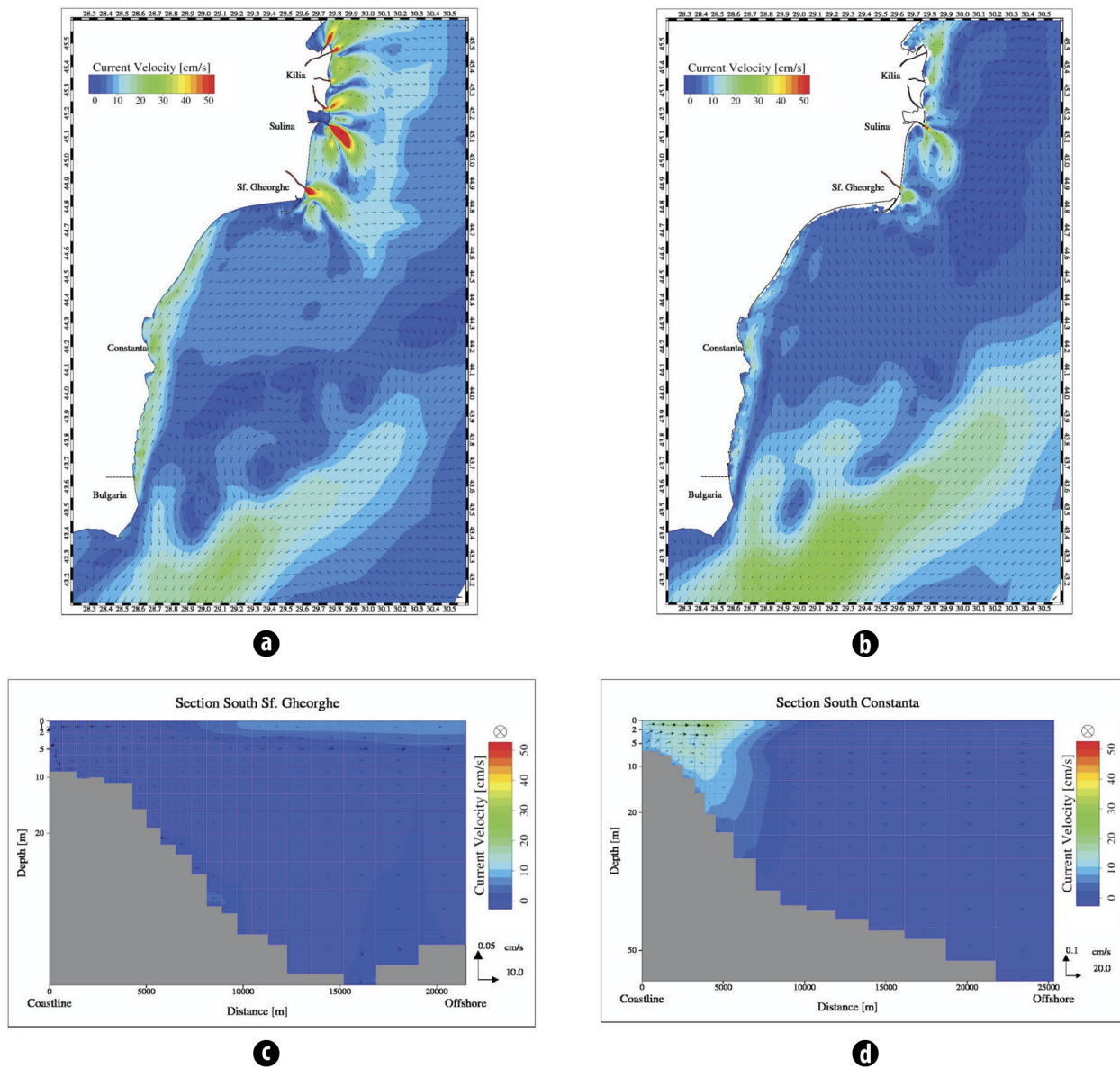


Fig. 19. Distribution of currents for S wind and high discharge, winter season: **a)** in the surface layer; **b)** at 5 m deep; **c)** cross-section located South of the Sf. Gheorghe mouth; **d)** cross-section located South of Constanta

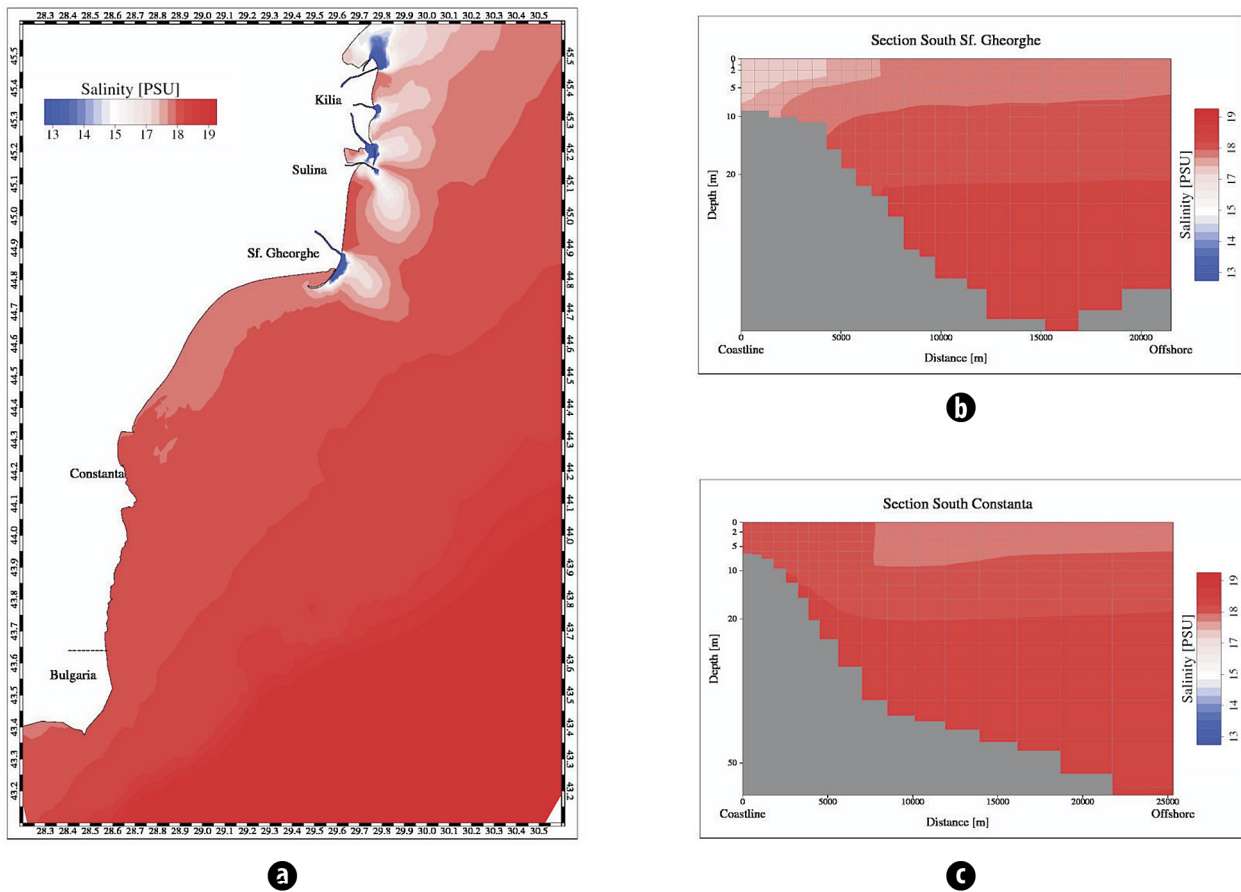


Fig. 20. Distribution of salinity for S wind and high discharge, winter season: **a)** in surface; **b)** cross-section located South of the Sf. Gheorghe mouth; **c)** cross-section located South of Constanța

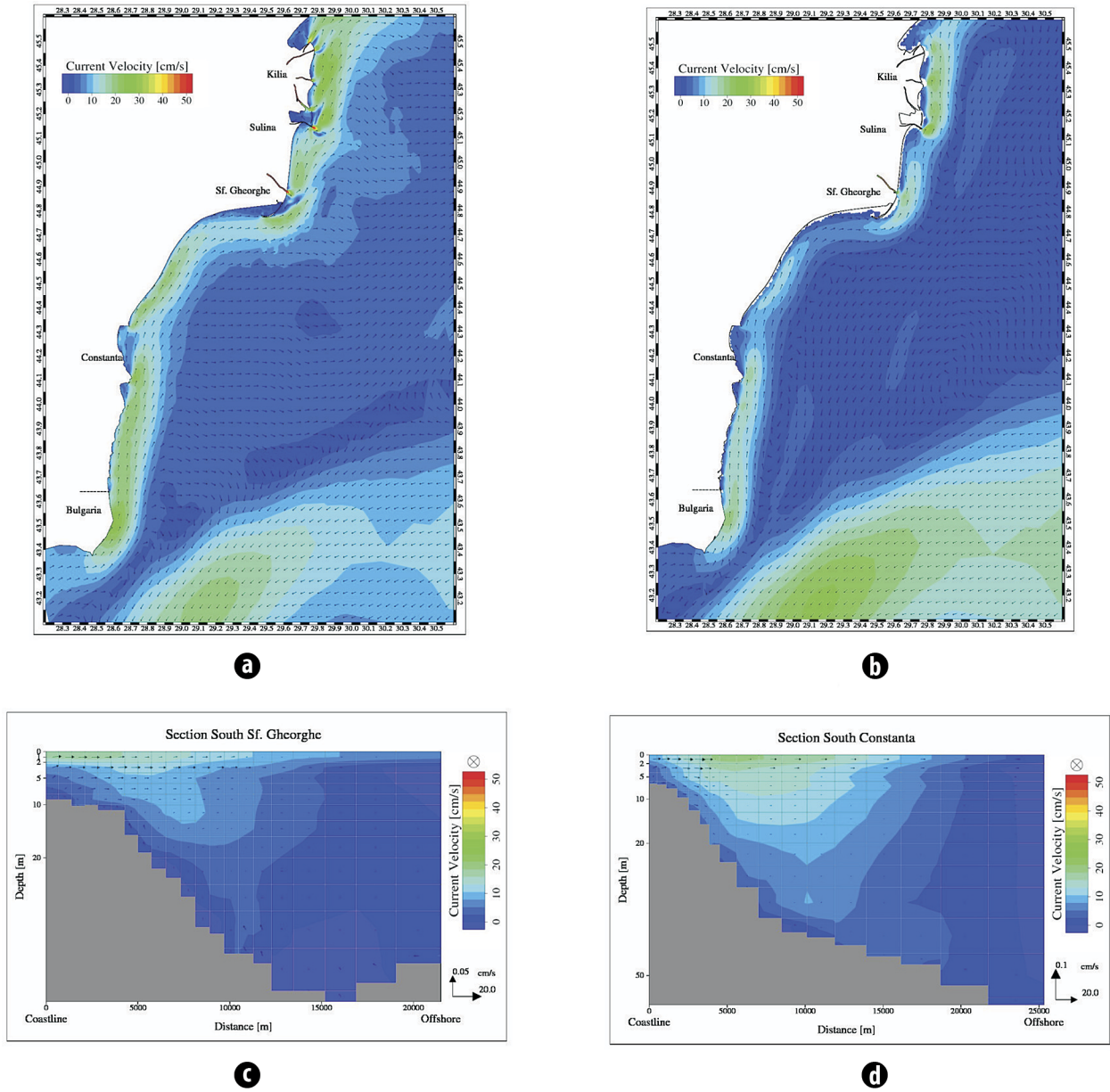


Fig. 21. Distribution of currents for S wind and low discharge, summer season: **a)** in the surface layer; **b)** at 5 m deep; **c)** cross-section located South of the Sf. Gheorghe mouth; **d)** cross-section located South of Constanța

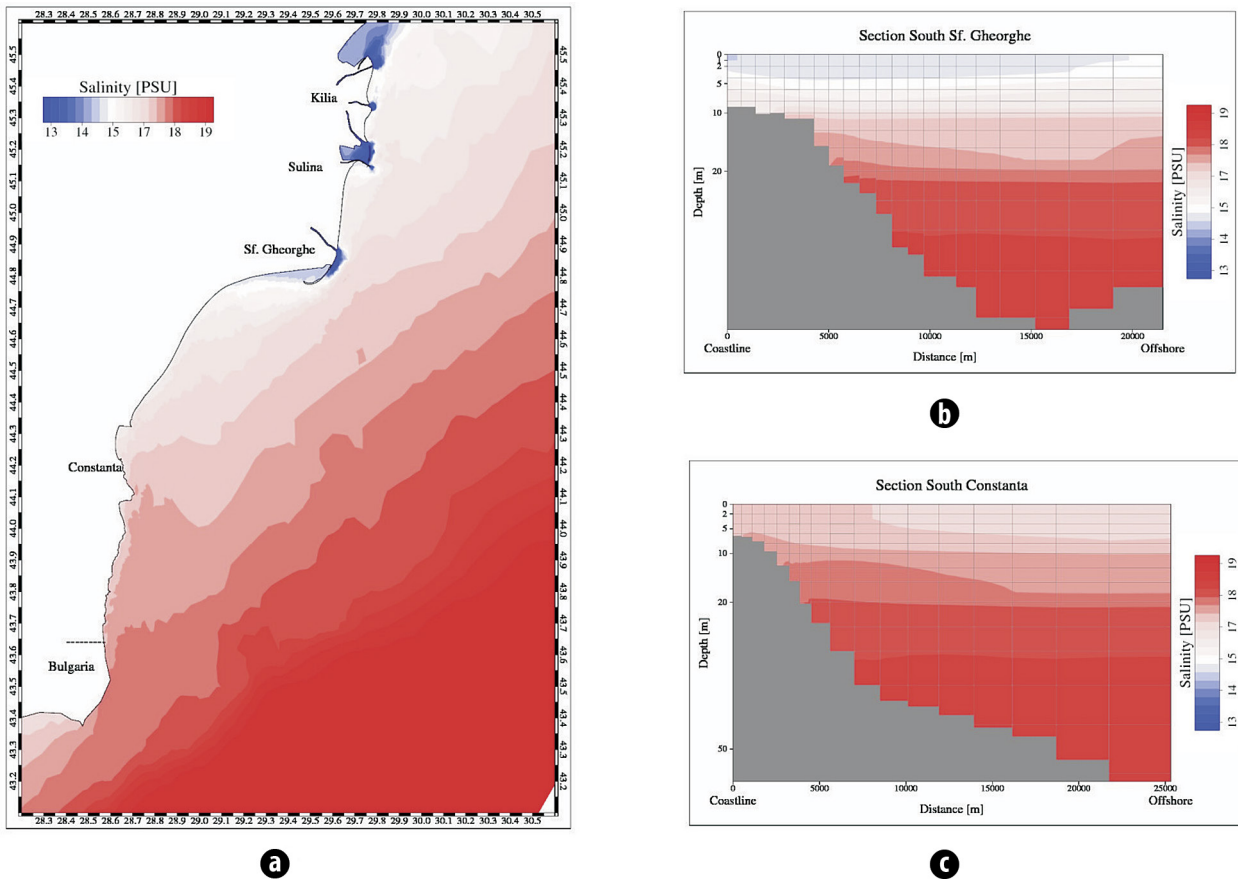


Fig. 22. Distribution of salinity for S wind and low discharge, summer season: **a)** in surface; **b)** cross-section located South of the Sf. Gheorghe mouth; **c)** cross-section located South of Constanta

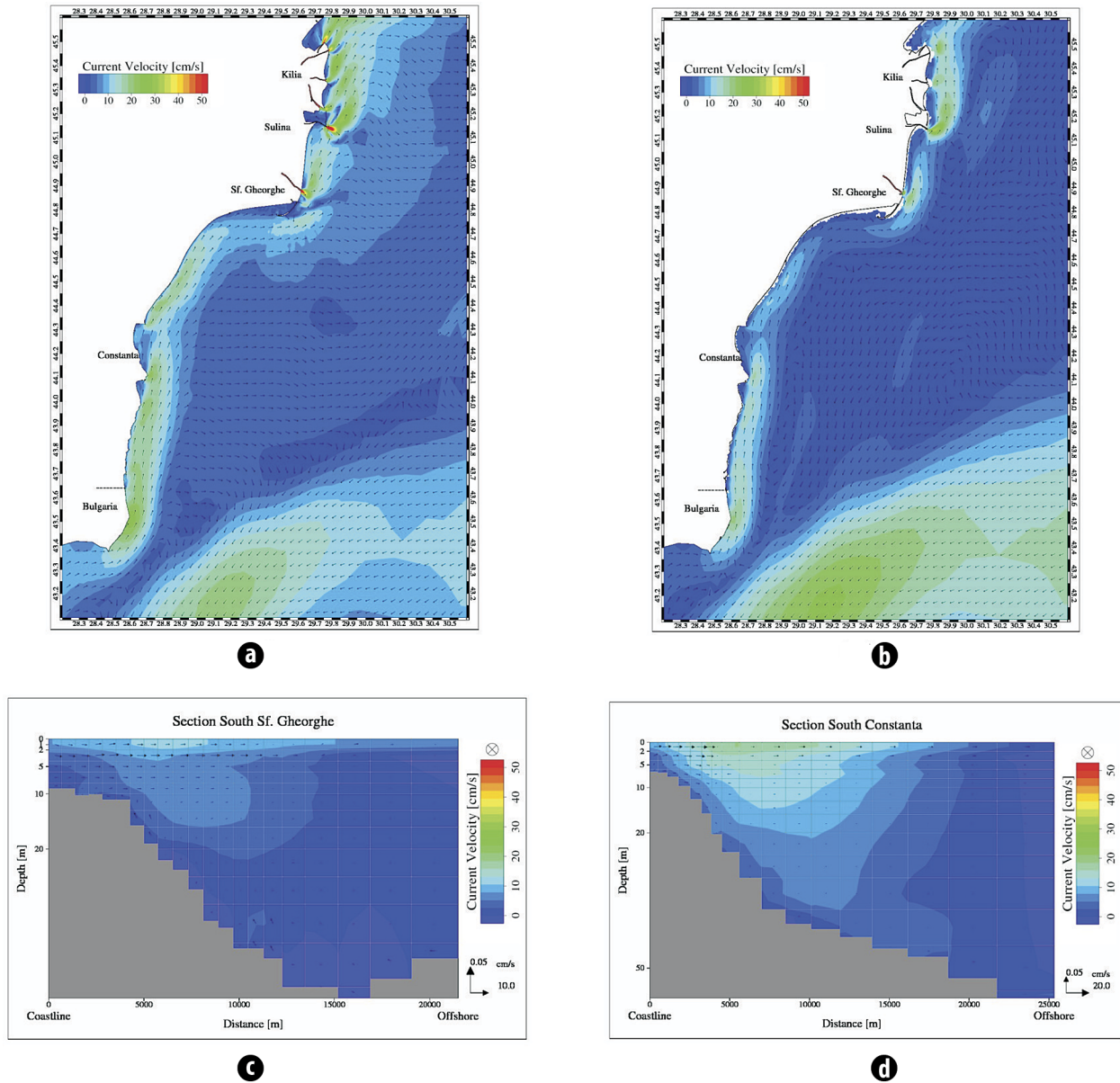


Fig. 23. Distribution of currents for S wind and medium discharge, summer season: **a)** in the surface layer; **b)** at 5 m deep; **c)** cross-section located South of the Sf. Gheorghe mouth; **d)** cross-section located South of Constanța

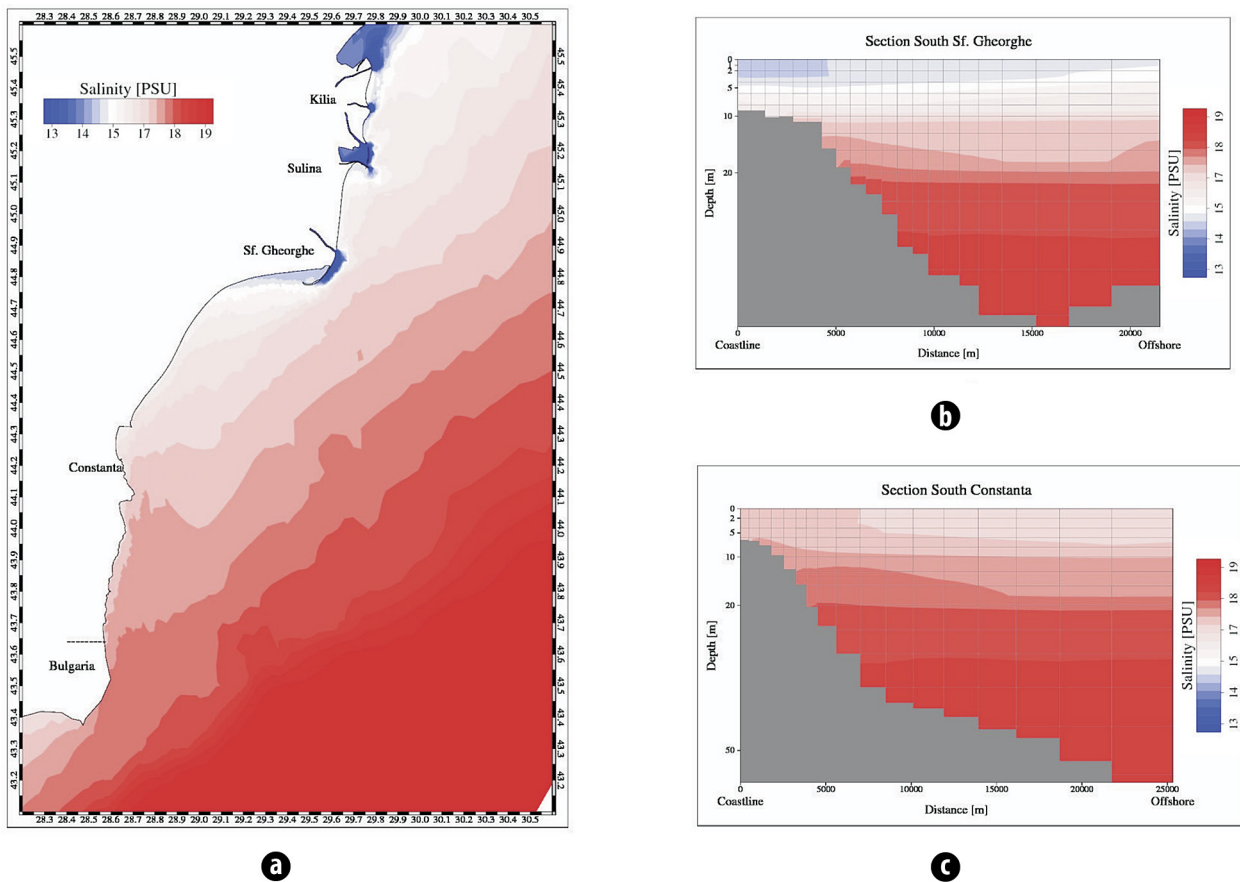
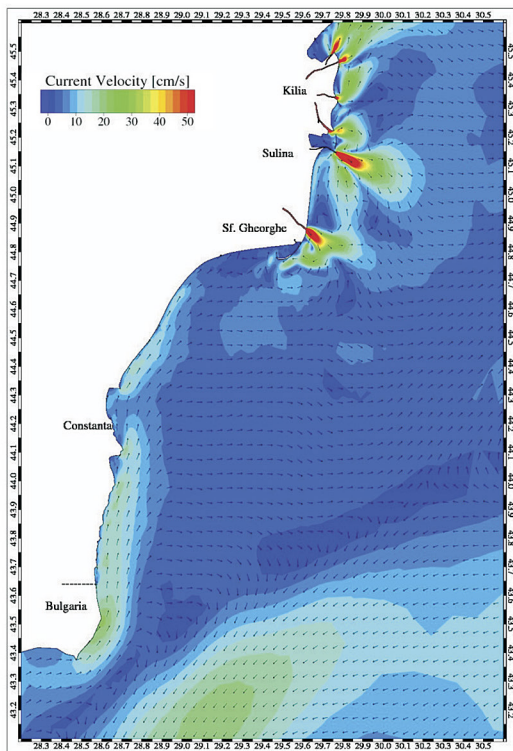
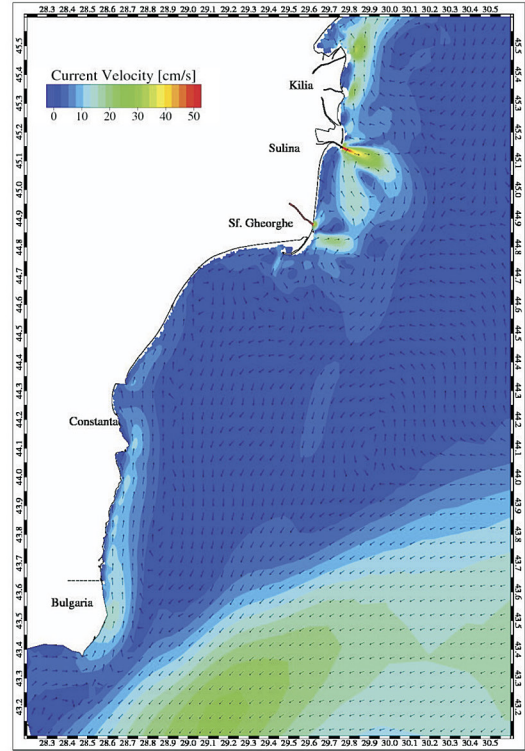


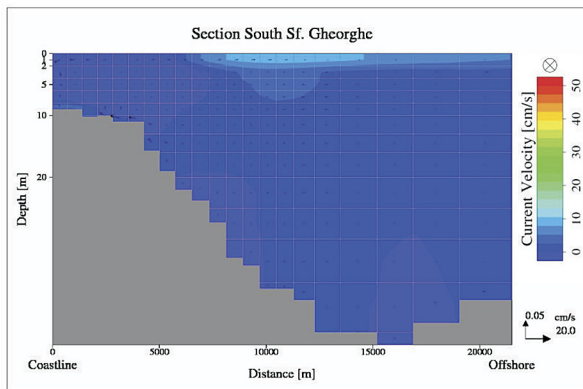
Fig. 24. Distribution of salinity for S wind and medium discharge, summer season: **a)** in surface; **b)** cross-section located South of the Sf. Gheorghe mouth; **c)** cross-section located South of Constanța



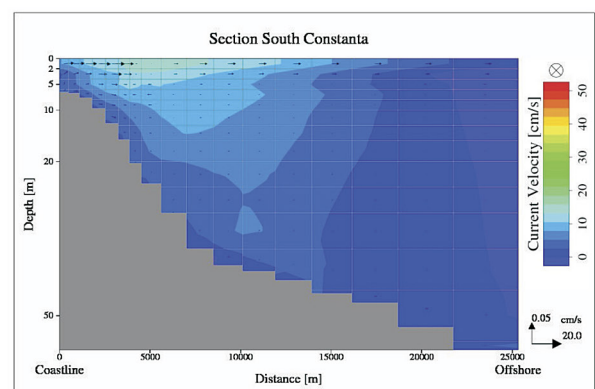
a



b



c



d

Fig. 25. Distribution of currents for S wind and high discharge, summer season: **a)** in the surface layer; **b)** at 5 m deep; **c)** cross-section located South of the Sf. Gheorghe mouth; **d)** cross-section located South of Constanța

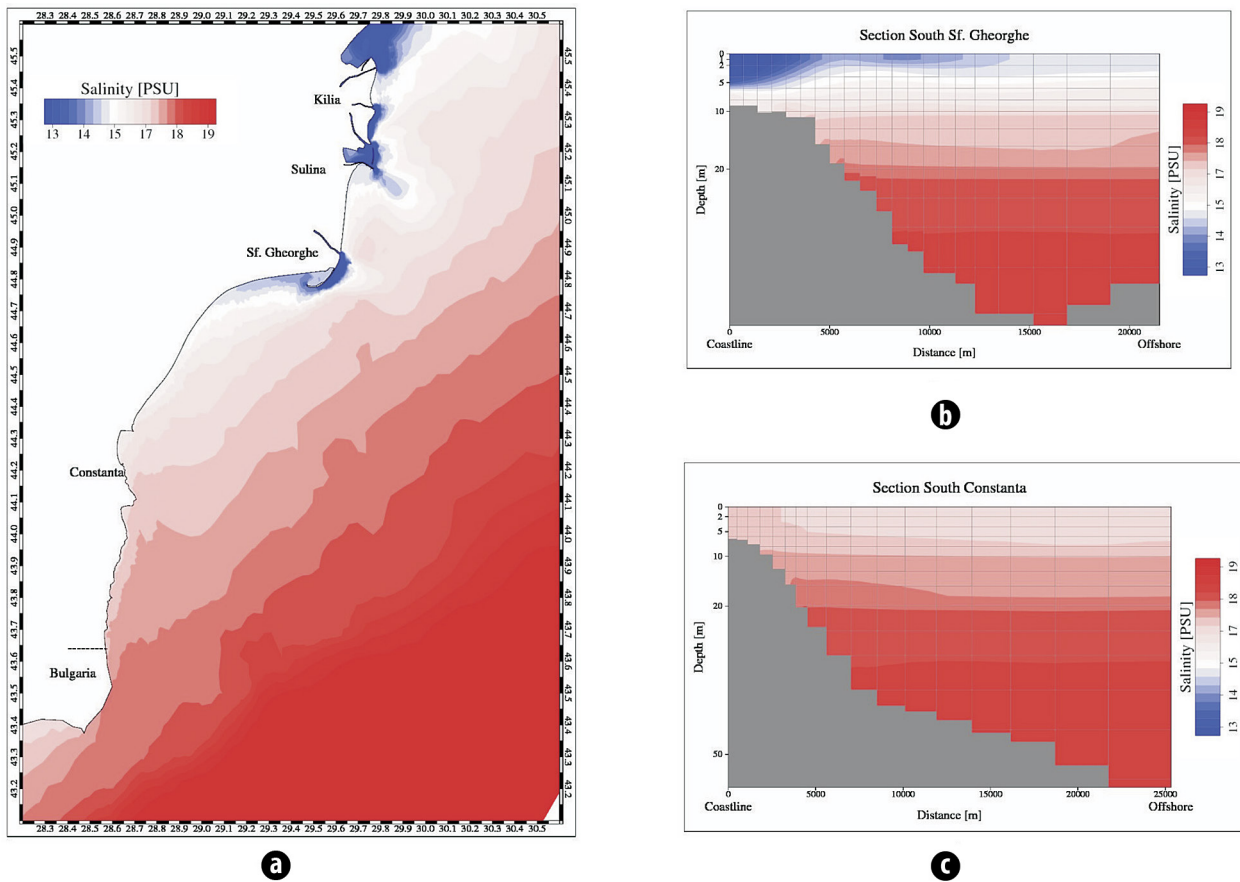


Fig. 26. Distribution of salinity for S wind and high discharge, summer season: **a)** in surface; **b)** cross-section located South of the Sf. Gheorghe mouth; **c)** cross-section located South of Constanța

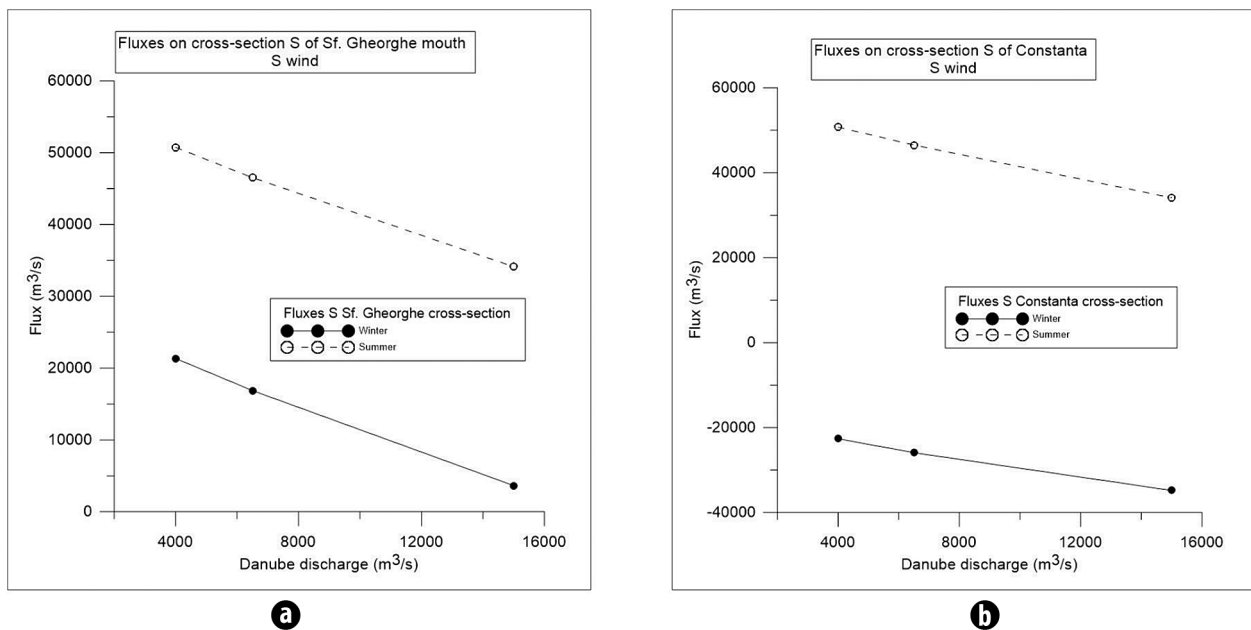


Fig. 27. Calculated fluxes for S wind on: **a)** the cross-section located South of the Sf. Gheorghe mouth; **b)** the cross-section located South of Constanța

Table 4. Winter and summer fluxes ($\text{m}^3\cdot\text{s}^{-1}$) calculated for the cross-section located South of the Sf. Gheorghe mouth for S wind

Danube discharge ($\text{m}^3\cdot\text{s}^{-1}$)	winter	summer
4000	12143.97	21343.12
6500	8611.49	16871.84
15000	- 2309.17	3626.59

Table 5. Winter and summer fluxes ($\text{m}^3\cdot\text{s}^{-1}$) calculated for the cross-section located South of Constanța for S wind

Danube discharge ($\text{m}^3\cdot\text{s}^{-1}$)	winter	summer
4000	- 22623.83	50740.39
6500	- 25904.45	46517.32
15000	- 34784.89	34124.63

The simulations for the winter and summer periods have been performed using the same values for the Danube discharge. The average wind velocities, calculated based on the available dataset, are slightly lower for the summer period. The main differences in the forcing are represented by the climatological distributions of temperature and salinity for the winter and summer periods.

At this stage of the study, we can state that the winter and summer fluxes, calculated on the analyzed cross-sections, are significantly influenced by the temperature and salinity distributions.

CONCLUSIONS

Average wind speed, based on the available monthly data from a 6 year period, and climatological values of temperature and salinity, have been used to force a hydrodynamic model developed on the Black Sea, both for winter and summer periods. Simulations have been run for low, medium and high Danube discharge. In our analysis, we have considered two frequent wind directions, Northeast and South, leading to strong coastal currents.

Wind from Northeast determines a strong southward current, which occurs, both in the surface layer and in deeper water. This current is stronger during the winter period. The salinity cross-sections emphasize the influence of the wind from Northeast, which tends to deepen the buoyant Danube water. The calculated fluxes are significantly higher for the winter period.

Wind from South determines a weaker Northward current, as it opposes the downdrift propagation of the buoyant Danube water. The stratification is weaker than with wind from Northeast.

For both wind directions considered, the salinity differs significantly for the winter and summer seasons.

In the case of wind from Northeast, the calculated fluxes are significantly higher for the winter period. In the case of wind from South, the calculated fluxes are significantly different for the winter and summer periods.

The winter and summer fluxes, calculated on the chosen cross-sections, are significantly influenced by the temperature and salinity distributions.

Even if this is a simplified approach, the results emphasize the main differences in the hydrodynamics of the Romanian coastal zone, between the winter and the summer periods.

ACKNOWLEDGEMENTS

This study has been carried out within the core project PN 16 45 02 02.

REFERENCES

- BAJO M., FERRARIN C., DINU I., UMGIESSER G., STĂNICĂ A. (2014). The water circulation near the Danube Delta and the Romanian coast modelled with finite elements. *Continental Shelf Research*, **78**(2014), p. 62-74.
- BELLAFIORE D., UMGIESSER G., CUCCO A. (2008). Modeling the water exchanges between the Venice Lagoon and the Adriatic Sea. *Ocean Dynamics*, **58**, p. 397-413.
- BONDAR C., ROVENTA V., STATE I. (1973). *Marea Neagră în zona litoralului românesc. Monografie hidrologică*. IMH Bucuresti, p. 1-516.
- BONDAR C., STATE I., CERNEA D., HARABAGIU E. (1991). Water flow and sediment transport of the Danube at its outlet into the Black Sea. *Meteorology and Hydrology*, **21** (1), p. 21-25, București.
- BONDAR C., PANIN N. (2001). The Danube Delta hydrologic data base and modelling. *Geo-Eco-Marina*, **5-6**, Bucharest-Constanta, Romania, p. 5-52.
- BONDAR C. (2006). Informații hidrologice privind fenomenul de tsunami în Marea Neagră inclusiv pe coasta României. *Hazard Natural: Evenimente Tsunami în Marea Neagră*. București, p. 92-102.

- DAN S., STIVE M., VAN DER WESTHUYSEN A. (2007). Alongshore sediment transport capacity computation on the coastal zone of the Danube Delta using a simulated wave climate. *Coastal Zone Processes and Management. Environmental Legislation – Geo-Eco-Marina*, **13**, p. 21-30.
- DAN S., STIVE M.J.F., WALSTRA D.J., PANIN N. (2009). Wave climate, coastal sediment budget and shoreline changes for the Danube Delta. *Marine Geology*, **262**, issues **1-4**, p. 39-49.
- DE PASCALIS F., UMGIESSER G., ALEMANNO S., BASSET A. (2009). Numerical model study in Alimini Lake (Apulia Italy). *Sedimentary Processes and Deposits within River-Sea Systems – Geo-Eco-Marina*, **15**, p. 21-28.
- DE PASCALIS, F., PÉREZ-RUZAFÁ, A., GILBERT, J., MARCOS, C., & UMGIESSER, G. (2012). Climate change response of the Mar Menor coastal lagoon (Spain) using a hydrodynamic finite element model. *Estuarine, Coastal and Shelf Science*, **114**, 118-129.
- DINU I., BAJO M., UMGIESSER G., STĂNICĂ A. (2011). Influence of wind and freshwater on the current circulation along the Romanian Black Sea coast. *Geo-Eco-Marina* **17**/2011, p. 177-190.
- DINU I., BAJO M., LORENZETTI G., UMGIESSER G., ZAGGIA L., MAXIMOV G., STĂNICĂ A. (2013). Discussion concerning the current circulation along the Romanian Black Sea coast. *Geo-Eco-Marina* **19**/2013, p. 17-37.
- DINU I., UMGIESSER G., BAJO M., DE PASCALIS F., STĂNICĂ A., POP C., DIMITRIU R., NICHESU I., CONSTANTINESCU A. (2015).- Modelling of the response of the Razelm – Sinoe Lagoon System to physical forcing. *Geo-Eco-Marina* **21**/2015, p. 5-18.
- FERRARIN C., UMGIESSER G. (2005). Hydrodynamic modeling of a coastal lagoon: The Cabras lagoon in Sardinia, Italy. *Ecological Modelling*, **188**, p. 340- 357.
- FERRARIN C., RAZINKOVAS A., GULBINSKAS S., UMGIESSER G., BLIUDŽIUTĖ L. (2008). Hydraulic regime-based zonation scheme of the Curonian Lagoon. *Hydrobiologia*, **611**, p. 133-146.
- GIOSAN L., BOKUNIEWICZ H., PANIN N., POSTOLACHE I. (1999). Longshore Sediment Transport Pattern along the Romanian Danube Delta Coast. *Journal of Coastal Research*, **15** (4), p. 859-871.
- HALCROW UK ET AL. (2011). Coastal Dynamics and Sedimentology Studies. Master Plan "Protection and rehabilitation of the coastal zone"
- PANIN N. (1998). *Danube Delta: Geology, Sedimentology, Evolution*. Association des Sédimentologues Français, Paris, 65 p.
- PANIN N., JIPA D. (2002). Danube River Sediment Input and its interaction with the Mouth-western Black Sea. *Estuarine, Coastal and Shelf Science*, **54**, p. 551-562.
- PANIN N. (2003). The Danube Delta. Geomorphology and Holocene Evolution: a Synthesis / Le delta du Danube. Géomorphologie et évolution holocène: une synthèse. In: *Géomorphologie: relief, processus, environnement*, **9** (4), Paris, 247-262.
- SPĂTARU A. N. (1990). Breakwaters for the Protection of Romanian Beaches. *Coastal Engineering*, **14**, p. 129-146.
- STĂNICĂ A., DAN S., UNGUREANU G. (2007). Coastal changes at the Sulina mouth of the Danube River as a result of human activities. *Marine Pollution Bulletin*, **55**, p. 555-563.
- STĂNICĂ A., PANIN N. (2009). Present evolution and future predictions for the deltaic coastal zone between the Sulina and Sf. Gheorghe Danube river mouths (Romania). *Geomorphology*, **107**, 41-46.
- STĂNICĂ A., DAN S., JIMÉNEZ J.A., UNGUREANU G.V. (2011). Dealing with erosion along the Danube Delta coast. The CONSCIENCE experience towards a sustainable coastline management. *Ocean & Coastal Management*, **54**, 898-906.
- TESCARI S., UMGIESSER G., FERRARI C., STĂNICĂ A. (2006). Current circulation and sediment transport in the coastal zone in front of the Danube Delta. *Coastal Zones and Deltas - Geo-Eco-Marina*, **12**, p. 5-16.
- UMGIESSER G., MELAKU CANU D., CUCCO A., SOLIDORO C. (2004). A finite element model for the Venice Lagoon. Development, set up, calibration and validation. *Journal of Marine Systems*, **51**, p. 123-145.
- UMGIESSER G. (2010). *SHYFEM – Finite Element Model for Coastal Seas. User Manual*. ISMAR – CNR, Venice, Italy.
- UMGIESSER G., FERRARIN C., CUCCO A., DE PASCALIS F., BELLAFIORE D., GHEZZO M., BAJO M. (2014). Comparative hydrodynamics of 10 Mediterranean lagoons by means of numerical modeling. *Journal of Geophysical Research: Oceans* **119** (4), p. 2212-2226.
- UNGUREANU G., STĂNICĂ A. (2000). Impact of human activities on the evolution of the Romanian Black Sea beaches. *Lakes & Reservoirs: Research and Management*, **5**, p. 111-115.
- VESPREMEANU-STROE A., CONSTANTINESCU Ș., TATUI F., GIOSAN L. (2007). Multi-decadal Evolution and North Atlantic Oscillation Influences on the Dynamics of the Danube Delta shoreline. *Journal of Coastal Research*, **SI 50** (Proceedings of the 9th International Coastal Symposium), p. 157-162.
- YANKOVSKY A.E., LEMESHKO E. M., ILYIN Y. P. (2004). The influence of shelf-break forcing on the alongshelf penetration of the Danube buoyant water, Black Sea. *Continental Shelf Research* **24**, p. 1083-1098.

